ИНСТИТУТ ЯДЕРНОЙ ФИЗИКИ СО АН СССР

O.K. Vorov

COLLECTIVE QUADRUPOLE EXCITATIONS OF SPHERICAL NUCLEI IN THE FRAMEWORK OF NONLINEAR VIBRATION MODEL. II. COMPARISON WITH EXPERIMENT

PREPRINT 86-170

НОВОСИБИРСК
1986

ABSTRACT

The even-even isotopes of palladium as well as ruthenium are considered in the framework of the model developed in the previous paper. Detail comparison of the spectroscopic data with the model calculations is carried out. The model has six phenomenological parameters fitted for each nuclid independently. Results show an overall agreement with experiment. About ten E2 matrix elements and from twelve to fifteen energy levels for each nucleus were included in the analysis. Predictions are made concerning quantities to be measured. Comparison with different IBM versions is also performed. The agreement of IBM results with experiment is not better and in many cases even worse than that achieved in the present model. Perspectives of the model concerning its further developments as well as applications to other regions of the periodical table are briefly discussed.

1. INTRODUCTION

In the previous paper [50] [1] has considered the model of nonlinear vibrations having be applied to description of the low-lying quadrupole collective excitations in soft spherical nuclei. The model is a straightforward generalization of the QAAM (quartic anharmonicity + angular momentum) model discussed earlier (Ref. [16]). In Ref. I an alhorithm was developed of calculating eigenvalues as well as eigenfunctions of the collective Hamiltonian

$$H=\frac{1}{2}\sum_{\mu}\pi_{\mu}\pi_{\bar{\mu}}+\frac{\overset{0}{\omega}{}^2}{2}\sum_{\mu}\alpha_{\mu}\alpha_{\bar{\mu}}+\frac{\lambda}{4}(d^{(+)4})_{00}+$$
$$+X^{(3)}\sum_{\mu}(d^{(+)2})_{2\mu}d^{(+)}_{\bar{\mu}}+\sigma J(J+1)\,, \qquad (1)$$

where the dimensionless collective variables α_μ and π_μ are connected with the quadrupole boson creation d^+_μ and destruction d_μ operators by means of relations

$$\alpha_{\mu}=\frac{1}{\sqrt{2}}(d_{\mu}+(-1)^{\mu}d^{+}_{-\mu})\equiv\frac{1}{\sqrt{2}}d^{(+)}_{\mu}\,, \qquad (2a)$$

$$\pi_{\mu}=\frac{i}{\sqrt{2}}(d_{\mu}-d^{+}_{\bar{\mu}})\equiv\frac{i}{\sqrt{2}}d^{(-)}_{\mu}\,, \qquad (2b)$$

$$d_{\bar{\mu}}=(-1)^{\mu}d_{-\mu}\,. \qquad (2c)$$

Here the symbol $(\quad)_{JM}$ as usual means the coupling to the corres-

[1] It would be below referred as I.

ponding angular momentum. The quadrupole operator for a calculation of E2 matrix elements is chosen in the form

$$T_\mu^{(E2)} = d_\mu^{(+)} + \varkappa((d^{(+)2})_0 d^{(+)})_{2\mu} + q\,(d^{(+)2})_{2\mu} +$$

$$+ q'(d^{(-)2})_{2\mu} + \frac{k}{2}([J, d^{(-)}]_+)_{2\mu}\,, \qquad (3)$$

in accordance with the microscopic consideration (see I.)

There are many nuclei in the periodical table which could be attributed to soft spherical ones. One usually uses geometrical properties of spectra as a critherion for such an attribution (see, for example, [1, 2, 4]). Actually, all nuclei which have a low-lying collective excitations but not manifest pronounced rotational-like spectra should be regarded as soft spherical ones. In such nuclei the members of «two-phonon» triplet 2^+ and 4^+ are slightly splitted and higher phonon multiplets are visible. Following the IBM-language, the regions of periodical table ascribing to SU(5) and O(5) symmetries have been included in consideration (i.e. isotopes of Se, Ge, Zn, Kr, Mo, Sr, Ru, Pd, Cd, Te, Xe, Ba, Ce, Pt). As typical representatives, ruthenium and palladium isotopes were choosen for analysis in present paper because of abundance of experimental data [5, 11—14, 17—20, 28—34, 38—42]. On the other hand, these nuclei used to be a test for various collective models [2, 10, 17, 18, 26, 27], particularly, the different versions of the IBM [26, 32, 32, 52]. It provides us an opportunity to compare the results of the anharmonic vibration model (AVM) with those obtained in previous models. As for the data on other nuclei, the author hopes to discuss them in subsequent papers [46] .

In I the analytical expressions for energies and E2 matrix elements as the functions of model parameters $\mathring{\omega}^2/\lambda^{2/3}$, χ, σ, $\varkappa$, q, q' are derived (see I) but one should use the simple computer code to fit the parameters and perform the comparison with experiment because corresponding formulas are rather complicated.

2. THE PROCEDURE OF THE CALCULATION

As it could be seen from the formulas (1), (3) one has six parameters to be fitted, three of those ($\mathring{\omega}^2/\lambda^{2/3}$, χ, σ) being of dynamical nature influence wave functions and all matrix elements, and another three ($\varkappa$, q, q') are essential to the E2-values only.

Since the experimental uncertainties for the energy values are negligibly small being compared to those for E2-matrix elements it seems reasonable to adopt the following routine of fitting.

a) Energy values for all known collective levels are fitted according to the standard band classification (as in Ref. [2]) by using three dynamical parameters which would be thus optimized. The optimization procedure is based on the standard least square method.

b) The values of parameters deduced at the first stage as well as the additional three parameters which would be fitted at this second stage are used in a procedure of calculating E2 matrix elements. The usage of the least square method is complicated at this stage because of experimental errors bars for transition probabilities and difference of results of various experimentalists. Therefore one has to be satisfied in many cases by a visual comparison with the complex set of data.

It should be pointed out that all the six parameters used are fitted for each isotope independently so the set of adopted values along the chain of isotopes contains some important information on collective nuclear motion. These values are to be calculated in the selfconsistent microscopic theory.

As it has already been mentioned in I. the parameters q and q' in operator $T^{(E2)}$ are small being essential especially for the calculation of the weak transition probabilities and quadrupole moments. As for the parameter $\varkappa$ it is specific for our model and modifies significantly all enhanced transition probabilities. Therefore, in a simplified version of the model one has three parameters of dynamical type and one more , $\varkappa$, for $T^{(E2)}$ matrix elements. Such an approximation has been adopted in calculations for selenium isotopes giving a good agreement with experiment. Nevertheless, the full set of parameters is used in the present paper to investigate all the possibilities of the model in its unrestricted form.

3. ENERGY SPECTRA

a) Yrast bands.

We show in Figs 1 and 2 the experimental spectra of the Yrast-bands in Ru and Pd isotopes and compare them with the results of calculations in the AVM and with those of the IBM-1 (Ref. [31]) and for IBM-2 (Ref. [26]). One can see that in spite of a general good agreement, the description of high-spin states, i. e.

8^+ and 10^+, in the IBM is not satisfactory. This feature is typical for all the IBM-calculations (see, for example, Refs [6, 7, 25, 29]). One usually ascribes this to the non-collective components of these states [25, 29, 31, 53] being probably mixed essentially with two-quasiparticle ones. Such a viewpoint based on the shortcomings of description of high-spin states in IBM is now frequently found, preventing the attempts to interpret the high-lying exciting states in the framework of collective boson models. The striking agreement obtained in the present model makes the hypothesis concerning the noncollective nature of those states unlikely. We shall show later that the description of other data (i. e. side-band states energies and transition probabilities) is also very good.

b) Side-bands.

In Figs 3 and 4 the energies of side X- and Z-bands are plotted being compared to the results of model calculations. One can see a good overall agreement for the AVM case, while an essential discrepancies are found for the IBM-results oversetimating the experimental $E_{5_1^+}$ and $E_{6_1^+}$ values. The only perceptible disagreement with the AVM prediction is observed for the quantity $E_{2_2^+}$ in ^{102}Pd.

The «three-phonon» level 3^+ treated as a head of the Z-band consisting of states with the odd angular momentum seems to be of great interest [33]. In fact, all the collective boson models predict the only 3^+ state placed at about $\leqslant 2$ MeV. The description of these states is crucial for testing the purity of collective quadrupole excitations and the validity of the whole approach. The results presented at Figs 5, 6*a* evidently show that the AVM is able to describe the placement of 3^+ states with a high accuracy. The predictions of the IBM-2 overestimates systematically the experimental values (this is due to the special choise of parameters destined to push up the unobserved states of mixed symmetry predicted by the model, see Ref. [26]). The same is valid for the IBM-1 (see [31], [29] and References therein).

Note that description of 3^+-states in the framework of the microscopical BET (Boson Expansion Technique) appears to be reasonably good (Ref. [33]). This approach is close physically to the AVM, but unfortunately cannot considered, at its current status, as completely selfconsistent theory.

An additional test of validity of the collective boson model is provided by the excited 0^+ states discussed below in detail. The first excited 0^+-states in this nuclear region, in contrast to the platinum

isotopes, appear to be «two-phonon»-like ones beloning to the β-band and having quantum numbers $v=0$, $n=1$ (see I). The second excited 0^+ state is proposed to have quantum numbers $v=3$, $n=0$ thus being placed at about $3E_{2_1^+}$. The Figs 5 and 6,*b* as well as corresponding parts of Figs 7 and 8 convince one that the AVM gives a reasonably good description of the «fine-structure» of 0^+-states while the IBM-versions hardly do.

c) β-band.

The excited 0-states which give rise to the β-band are of great importance being a most difficult feature to explain (see refs. [9, 10, 26, 30, 31, 33, 43, 54]). For example, there are extremely low-lying 0-excitations in some isotopes of Se, Ge and Mo. The high-lying 0^+ states in xenon, platinum and osmium isotopes were interpreted in the O(6) limit of the IBM. In the present model, the universal description of the excited 0^+-states is achieved on the basis of anharmonicity concept. In such a framework, the high-lying 0^+ states are considered as a result of the strong quartic anharmonicity in the hamiltonian (1) especially for the parameter $\mathring{\omega}^2/\lambda^{2/3}$ being of negative sign. Particularly, it is shown in Ref. [46] that one can describe all the features of excited 0^+-states in isotopes $^{194-198}$Pt by means of smooth variation of the parameter $\mathring{\omega}^2/\lambda^{2/3}$ from one nucleus to another.

As for the palladium and ruthenium isotopes, one could see from Figs 7 and 8 that the AVM gives an excellent description of E values meanwhile the IBM-2 fail to reproduce the $E_{0_2^+}$ dependence on the neutron number . The decay properties of 0^+ states also have been described in AVM very good (see sec. 4).

The third excited 2_3^+ states are the only well pronounced members of the beta-band in the experimental pattern (except the 0^+ states). In the AVM framework, these states have quantum numbers $v=1$, $n=1$ being of «three-phonon» nature. The energy of the 2_3^+ state is rather sensitive to the strentgh of the quartic and cubic interaction (see I, sec. 5), providing, as a consequence, an additional possibility to determine the anharmonicity scale from the comparison with experiment. The remarkably good description of β-band members by the AVM was found as distinct from the IBM-1 or the IBM-2 (see Figs 7 and 8)[2)]

[2)] It was the discrepancy between theory and experiment for those quantities that inclined the authors of Ref. [26] to appeal to the probable non-collective nature of 0^+ states.

As a whole, basing on the comparison performed in this section, ne can conclude that the AVM provides a good description of nergy spectra of palladium and ruthenium isotopes succeeding to eproduce the fine features of experimental patterns.

It should be stressed that the agreement obtained in the present nodel being better than that for the IBM is achieved by use of three fitted parameters only. The parameter number is essentially less than in the case of the IBM (especially IBM-2, where this number is too large forsing to fix some of them in rather arbitrary manner). One shouldn't be surprised that the agreement for the IBM-1 might be for some states better than for the IBM-2 (as it could be seen from Figs 1—8). It could be easily understood since the authors of Refs [31, 32] havn't fitted all the set of data so some of quantities (for example, quadrupole moment expectation values) are in disagreement with the experiment being calculated by use of parameters adopted by the authors.

d) For some individual cases the unusual abundance of experimental data is available, namely, for ^{104}Ru and ^{110}Pd. Strikingly enough, the locationt of all the levels identified experimentally up to energy about 3.5—4. MeV (i. e. 16—18 levels) is reproduced with a high precision by the AVM-calculations.

The spectra of Yrast-band and side-bands in ^{104}Ru are presented respectively, in Figs 9 and 10 being compared with the results of AVM-calculations as well as those of IBM-2 and IBM+g (the sophisticated version of the IBM including the g-boson with $l=4$) from Refs [17] and [18]. Going along the columns a-d one can to trace a gradual improvement of the AVM results following from the pure vibrator to the QAAM and then to the version with fitting of the quartic anharmonicity strength and, to this end, to a full three-parameter fit with the cubic anharmonicity being included. Note that for the Yrast-band, the QAAM is certainly enough to describe the whole information with high accuracy. As for the IBM-versions, IBM-1 and IBM-2 do provide the description of less quality for the number of parameters fitted being larger (about $4\div5$) than in the AVM.

The second remarkable nucleus, ^{110}Pd, is presented in Fig. 11 where both the energy levels and E2 transition probabilities are shown. The agreement in the level pattern looks quite impressive, especially for the higher members of side-bands. Note that the main E2-properties of these nuclei are reproduced by the model remarkably good too (see Figs 23—25).

To compare the accuracy of description of energy spectra of AVM and IBM, for the latter the three-parameter formulae of the IBM-SU(5) limit from Ref. [2] was used by the author to fit the values $E_{J^+}/E_{2_1^+}$ for all the parameters being optimized independently. The results for the averaged squared deviations from the experiment are plotted in Fig. 12 and compared with those for the QAAM and AVM calculations.

4. ELECTROMAGNETIC QUADRUPOLE TRANSITIONS

a) Enhanced transitions ($\Delta N=1$).

The results of calculations for relative E2 transition probabilities with $\Delta N=1$ are presented at Figs 13—16 in comparison with experimental ones and with IBM-2 (Ref. 26]) and IBM-1 (Ref. [32]) predictions.

One sees a general good agreement with experimental data for both the chains of isotopes, the quality of description is roughly speaking equivalent for models used. Nevertheless, the AVM reproduces the behaviour of $B(\mathrm{E2};\ 0_2^+\to2_1^+)$—values versus neutron number noticeably better than IBM versions, as it can be seen from Figs 15 and 16 (see next sec.).

Unfortunately, the experimental information concerning the Yrast-band transitions in Ru—Pd region is still incomplete. The extensive investigation of palladium isotopes has just been begun by D. Cline and collaborators (Refs [28] and [41]). The isotope Ru has been studied in detail by J. Stachel et al. [17, 18] where a great deal of important information concerning the E2 matrix elements has been obtained.

The predictions for $B(\mathrm{E2})$ values along the Yrast-bands basing on the values of parameters optimized by fitting the known transition probabilities are given in Figs 26 and 27. The predictions of other models are also presented where they were made. For the IBM-1 case, the author made calculations using the IBM-parameters adopted in Ref. [32].

The ratio $B(\mathrm{E2};\ 3_1^+\to4_1^+)/B(\mathrm{E2};\ 3_1^+\to2_2^+)$ provides a simple test of O(5) symmetry breaking (see I). In the case of O(5), it should be equal to 2/5 as well as in pure vibrational limit, deviations are due to the symmetry violation. It is the cubic interaction $H^{(3)}$ in present case that breaks the O(5)-invariance. One sees from Figs 19 and 20

that the deviations aren't essential for palladium isotopes where one has allmost a pure O(5) symmetry. The cubic corrections are substantial for ruthenium isotopes, especially for ^{102}Ru (see Table 2) for which the deviation appears to be maximum.

Another test of O(5)-conservation concerns with the crossover transitions (those for which $\Delta N=2$), see below.

b) Cross-over transitions.

The strongly hindered E2-transitions with the selection rule $\Delta N=2$ have been observed in all typical soft nuclei corresponding $B(\mathrm{E2})$ values being reduced by factor 10^{-2} as compared with those for enhanced transitions. As mentioned in I, these are caused in the AVM picture by incorporation of cubic anharmonicity as well as by the third and fourth terms in the $T^{(\mathrm{E2})}$-operator (3). Figs 17, 18 (upper part) and 21, 22 (lower part) illustrate the description of those quantities in terms of boson models. Ignoring the conflicting character of some experimental results, one sees as a whole satisfactory agreement for all the versions (especially keeping in mind the smallness of values considered). The AVM, with the E2-operator in form (3), predicts also very hindered transitions with $\Delta N=3$ caused by the second term in (3). Those quantities are of order $10^{-3}-10^{-1}$ compared to $B(\mathrm{E2};\ 2_1^+\to 0_1^+)$, being very sensitive to many minor effects, for example, to additional terms in the $T^{(\mathrm{E2})}$-operator in the next adiabatic order. So the quantitative predictions for $B(\mathrm{E2};\ 2_3^+\to 0_1^+)$ presented in Figs 19, 20,*c* should be considered as preliminary. Where the empirical information exists, corresponding values are small correlating in some cases with those predicted, at least in order of magnitude. Apparently, one should wait for more experimental data which would give basis for detailed conclusions concerning the fine structure of the E2-operator.

d) Intramultiplet transition probabilities with $\Delta N=0$ appear to be of a special interest since they are connected with the same physical origin as the cross-over transitions. One could expect all those probabilities being small, however, a geometrical enhancement exists for some of E2-matrix elements linking the members of the same multiplet. One can easy obtain the following simple relationship between the matrix elements of the cross-over $2_2^+\to 0_1^+$-transition, the first excited state quadrupole moment, $Q_{2_1^+}$, the $4_1^+\to 2_2^+$ transition and the $0_2^+\to 2_2^+$ transition supposing all those to be due to the cubic anharmonicity only:

$$|0_{2_1^+}|:\sqrt{B(0_2^+\to 2_2^+)}:\sqrt{B(4_1^+\to 2_2^+)}:\sqrt{B(2_2^+\to 0_1^+)}=$$
$$=\sqrt{\frac{16\pi}{70}}:1:\frac{8}{49}:\frac{1}{16} \qquad (4)$$

It is evident from eq. (4), that the value of $B(0_2^+\to 2_2^+)$ must be the same order of magnitude as $Q_{2_1^+}$. Since the latter is known experimentally to be of order of unity (compared to the $B(\mathrm{E2};\ 2_1^+\to 0_1^+)$) for many nuclei, the former is of the same order too in spite of the values $B(4_1^+\to 2_2^+)$ and $B(2_2^+\to 0_1^+)$ being small (typically 10^{-2}). The same is approximately valid for the corrections to E2-operators (eq. (3)) being accounted too.

Figs 19 and 20*a*, *b*) illustrate that such predictions are in reasonable agreement with the empirical quantities known for palladium isotopes though the predicted $B(\mathrm{E2};\ 4_1^+\to 2_2^+)$ value for $N=62$ goes over the empirical one. Since there was not any predictions presented in Ref. [32] for the IBM-1 version the author has carried out IBM-calculation using the same values of fitted parameters as in Ref [32]. The results are 0.304, 0.253, 0.107, 0.459 and 0.033 (e^2bn^2) for the chain of Pd isotopes respectively being in rather bad agreement with experiment for their magnitudes leap from one nucleus to another.

e) Quadrupole moment expectation values.

Only quadrupole moments of the first excited 2^+ states are measured systematically for both the chains of isotopes. The corresponding values as well as model calculations are presented in Figs 17, 18,*b*. It is evident that experimental values are generally of order $\sqrt{B(E2;\ 2_1^+\to 0_1^+)}$. Taking into account the anharmonic corrections one can reproduce these large values consistently. One see that for some nuclei IBM-2 calculations correlate with the experimental data better than those of the AVM, in latter case the agreement might be improved by inclusion of additional fitted parameters. The IBM-1 calculations performed with the values adopted by the authors of Ref. [32] failed to reproduce the behaviour of $Q_{2_1^+}$ as a function of neutron number.

It should be mentioned that the experimental uncertainties as well as discrepancies between the results by different authors remain to be rather substantial.

5. DECAY PROPERTIES OF EXCITED 0^+-STATES

It is well known [26, 32, 47] that the transitions in which the largest discrepancy is encountered between theory and experiment are those connected with the 0_2^+ states. In fact, the pure vibrational model [1] fail to reproduce the values of ratios $B(E2; 0_2 \to 2_1)/B(E2; 2_1 \to 0_1)$ and $B(E2; 0_2 \to 2_2)/B(E2; 2_1 \to 0_1)$. Experimentally, the former usually is essentially less than harmonic oscillator value 2. The latter is about 2—2.5 for the observed transitions meanwhile the vibrational model predicts zeroth value for this ratio. It makes someone to conclude that these 0^+ states are of non-collective nature [9, 18, 48, 52]. IBM-predictions as well as results of boson expansion technique are for many cases in better agreement with experiment [26, 32], nevertheless, some discrepancies are conserved.

The AVM with the strong quartic anharmonicity predicts the 0^+ states to exhibit the features distinguishing from those of other terms of the two-phonon triplet $(2_2^+, 4_1^+)$, for the latter belong to the representation of O(5) with $v=2$, while the former belongs to the representation with $v=0$ (the same as ground state) giving rise of β-band and being spaced from vacuum state by the frequency of beta-vibrations, ω_β :

$$\omega_\beta = \frac{1}{2}\omega_0\left(5 - \frac{\overset{0}{\omega}{}^2}{\omega_0^2}\right), \tag{5}$$

as it can be seen from I, formula (10). This quantity is not equal to doubled ω_0, the one-boson excitation energy exceeding the latter for the strong quartic anharmonicity. In fact, one-boson excitation becomes more and more soft comparing to the «beta-vibrations» with the quantity decreasing.

The peculiar nature of the 0_2^+-states as a member of a β-band might be understood in another manner reasoning by analogy with the IBM . The hamiltonian H may be written in another form by use of the canonical scale transformation

$$\pi = \sqrt{|\overset{0}{\omega}|}\,\pi', \qquad \alpha = \frac{1}{\sqrt{|\overset{0}{\omega}|}}\alpha',$$

then

$$H = |\overset{0}{\omega}|\left\{\frac{1}{2}\sum_\mu \pi'_\mu \pi'_\mu \pm \frac{1}{2}\sum_\mu \alpha'_\mu \alpha'_\mu + \right.$$

$$\left. + X^{(4)}(\alpha'^4)_{00} + x^{(3)}(\alpha'^3)_{00}\right\} + \sigma J(J+1), \tag{6}$$

where the notations are equivalent to those used in Ref. [43] and connected to parameters $X^{(3)}$, $X^{(4)}$ by the following relations

$$\lambda = |\overset{0}{\omega}|^3 X^{(4)} \tag{7a}$$

$$X^{(3)} = 2\sqrt{2}\,|\overset{0}{\omega}|^{5/2} x^{(3)} . \tag{7b}$$

Considering the variables α', π', d' to be related to initial bosons with the energy equal to unity, one can find the expectation value of initial boson number operator N' in the true eigenstates $|v, n)$. One finds in the first approximation (see I) :

$$(v, n|N'|v, n) = \frac{1}{2}\left(\frac{\omega_v}{|\overset{0}{\omega}|} + \frac{|\overset{0}{\omega}|}{\omega_v}\right)(v+2n) + \frac{5}{2}\left(\frac{\omega_v}{|\overset{0}{\omega}|} + \frac{|\overset{0}{\omega}|}{\omega_v} - 2\right).$$

Thus even the ground state of the system contains d-boson pair condensate. The condensate power increases with the $\overset{0}{\omega}{}^2/\lambda^{2/3}$ depressing, and becomes especially substantional in the vicinity of $\overset{0}{\omega}{}^2 = 0$. This situation is similar to that in O(6) limit of IBM where the vacuum d-boson pair condensate also exists affecting all the observed quantities. Actually, the AVM with the only quartic anharmonicity does cover both SU(5) and O(6) limits as well as intermediate region, the vacuum d-boson condensate being regulated by the value of $\overset{0}{\omega}{}^2/\lambda^{2/3}$.

One can see from Figs 15, 16, 19 and 20,*a* that the AVM provides the best description of the decay properties of 0_2-states. In fact, the 0_2-states should be qualified as «two-phonon» states (i. e. ones with quantum numbers $v=0$, $n=1$). This assignment is strongly supported by the E2-transition properties and by the energy placement. The good agreement with calculated values for the energies of the 0_3-states confirms the assumption on their «three-phonon» nature with quantum numbers $v=3$, $n=0$. This is supported also by the relative smallness of $B(E2; 0_3^+ \to 2_1^+)$ values [52]. As for the nucleus ^{102}Pd, the situation is not so clear [41]. The states 0_2^+ and 0_3^+ occur at approximately same energy with the gap 34 keV. It is in conflict with the assumption for both them to be of the same collective structure since for that case anharmonicity will push them one

from another. On the other hand, the experimental value of $B(E2; 0_3 \to 2_1)/B(E2; 2_1 \to 0_1) = 0.39(10)$ for this nucleus [41] exceeds essentially the predicted by the AVM crossover-type value 0.04. It implies the strong mixing of states which can be the case in the AVM-framework if $\mathring{\omega}^2/\lambda^{2/3} = -6$ (see I) when the excited 0_2^+ and 0_3^+-states are closely placed at $E = 3.56\, E_{2_1}$. In this case, the more refined technique to calculate the properties of these states is required as well as an additional experimental information (especially on the quantities $B(E2; 0_3^+ \to 2_2^+)$ and E_{0_4}).

Removing this case, one could say that experimental systematics on 0^+-states in ruthenium and palladium isotopes is successfully described in the AVM.

6. PARAMETER VALUES AND PREDICTIONS

As already mentioned in sec. 2, all the six parameters $X^{(4)}$, $x^{(3)}$, σ, $\varkappa$, q and q' have been optimized for each nuclei independently. The values thus obtained are summarized in the Tables 1 and 2 where their reparametrization according to eqs. (7) is adopted (the sign of the quadratic term in the potential energy is noted). As a whole, one sees a smooth dependence of all values on the neutron shell occupation for both the isotopic chains.

Table 1

n	52	54	56	58	60	62
$X^{(4)}$	0.105 (−)	0.008 (+)	0.341 (+)	0.868 (−)	0.125 (−)	0.083 (−)
$x^{(3)}$	0.078	0.132	0.589	1.319	0.076	0.000
σ	−0.018	0.011	0.017	0.013	0.021	0.034
$\varkappa$	−0.220	−0.529	−0.180	−0.152	−0.157	
Q	0.040	0.034	0.082	0.053	0.055	
Q'	−0.002	0.000	0.018	0.004	0.023	

Table 2

n	54	56	58	60	62	64	66
$X^{(4)}$	0.253 (−)	0.675 (−)	0.125 (+)	0.007 (+)	0.084 (+)	0.084 (+)	0.095 (−)
$x^{(3)}$	0.428	0.339	0.237	0.063	0.000	0.000	0.000
σ	−0.003	0.011	0.018	0.024	0.019	0.026	0.019
$\varkappa$		−0.299	−0.314	−0.511	−0.191	−0.279*	
Q		−0.045	−0.043	−0.152	−0.159	−0.141*	
Q'		0.027	0.008	0.007	0.027	0.022*	

* These values are choosen by the extrapolation rather than the fitting procedure.

One can also trace the tendency for the values of $x^{(3)}$ to depress with the softness increasing (the quantity $\mathring{\omega}^2$ becoming negative) going to the middle of the neutron shell. Such a behaviour agrees with the microscopic evaluations (see I). As for the quasirotational parameter σ, its behaviour appears to be in the exact agreement with the regularities established in Refs [8, 16] for corresponding values going through the zero at about two or four neutrons beyond the closed shell. One should remember that in spite of respectively large values of parameter $x^{(3)}$ for some isotopes, the actual order of corrections induced by the cubic interaction is determined by χ, the latter being small due to the renormalization discussed in I. Those values are plotted in Fig. 28.

Speaking about the $T^{(E2)}$-parameters, one also have to note the smooth variation of their values from one nucleus to another. The hierarchy relations $|\varkappa| > |q| > |q'|$ based on the microscopical estimates (see I) are found to be the case, at any rate, in the region of nuclei considered.

Some irregularities occuring in the Tables 1 and 2 might be regarded to artefact of the fitting procedure, or they may indicate the real cases of sharp dependence on the shell occupation.

Basing on the parameters extracted, one can predict the value of quantities which should be measured but still aren't. In addition

to Figs 26 and 27 in the table 3 the predictions are summarized and various models are compared, namely, the IBM-1 and boson expansion technique (Refs [22, 23, 33]).

As it can be seen from the table 3, some energy levels belonging to the lowest multiplets are still unobserved, especially, the excited 0^+-levels.

7. SUMMARY AND CONCLUSION

In part I of this paper we have presented the theoretical scheme for the description of collective effects in even-even spherical and soft nuclei in the framework of the anharmonic vibration model. We have restricted ourselves by the softest quadrupole mode being of greatest interest. The model considered is constructed as a straightforward extension of the QAAM (quartic anharmonicity + angular momentum effects) having been successfully applied [16] to the description of even-even palladium isotopes. Besides the main nonlinearities, we also consider a cubic anharmonicity important for the detailed description of the experimental pattern. A general form of the E2-operator was used including, besides the main terms, the additional ones rising from the non-collective and non-adiabatic effects to be accounted. The simple closed-form analytical expressions are derived by means of perturbation theory for both the energies and E2 transition probabilities.

In the present part, II, the model is applied to the description of even-even ruthenium and palladium isotopes. The chains $^{96-106}$Ru and $^{100-112}$Pd are studied systematically, for about ten E2-matrix elements and twelve or fifteen energy values for each nucleus included in the analysis. Thus the almost complete set of experimental data known up to now have been used. A great deal of predictions is made concerning quantities having not yet been measured.

Comparison with the IBM-1 as well as IBM-2 results is also performed whereever it is available.

Particular attention was paid to the properties of those states which commonly appear the source of difficulties when described in collective models (such as excited 0^+-states). For these cases a reasonably good correspondence between experimental and theoretical quantities was obtained.

The main results of the study can be summarized as follows.

Table 3

Nucleus	Quantity	AVM	IBM-1	BET [33]
1	2	3	4	5
^{96}Ru	$E_{4_2^+}$	2.656	3.687	
	$E_{5_1^+}$	3.713	3.332	
	$E_{6_2^+}$	3.531	2.942	
	$E_{3_1^+}$	2.778	3.296	
	$E_{0_3^+}$	3.144		
	$E_{2_3^+}$	3.369	3.170	
	$B(0_2^+\to 2_1^+)$	3		
	$B(2_2^+\to 0_1^+)$	9		
	$B(0_2^+\to 2_2^+)$	1135		
	$B(4_1^+\to 2_2^+)$	5		
	$B(2_3^+\to 0_1^+)$	21	0.	
	$B(3_1^+\to 4_1^+)$	281		
	$B(3_1^+\to 2_2^+)$	643		
	$B(3_1^+\to 2_1^+)$	24		
	Q_{2_2}	9.5		
	Q_{4_1}	−9		
^{98}Ru	$E_{5_1^+}$	2.911	2.878	
	$E_{6_2^+}$	2.965	2.949	
	$E_{0_3^+}$	2.083	1.970	
	$B(0_2^+\to 2_1^+)$	294	1004	990
	$B(0_2^+\to 2_2^+)$	260	1205	
	$B(4_1^+\to 2_2^+)$	2	109	
	$B(2_3^+\to 0_1^+)$	44	0	7
	$B(3_1^+\to 4_1^+)$	401	260	380
	$B(3_1^+\to 2_2^+)$	904	1064	
	$B(3_1^+\to 2_1^+)$	44	33	46
	Q_{2_2}	17	−1	23
	Q_{4_1}	−17	58	−50

(*Continue*)

1	2	3	4	5
^{100}Ru	$E_{5_1^+}$	2.697	3.130	
	$E_{6_2^+}$	2.801	3.100	
	$B(0_2^+\to 2_2^+)$	2384	2403	
	$B(4_1^+\to 2_2^+)$	93	156	
	$B(2_3^+\to 0_1^+)$	3	0	12
	$B(3_1^+\to 4_1^+)$	481	556	
	$B(3_1^+\to 2_2^+)$	1462	838	
	$B(3_1^+\to 2_1^+)$	95	20	
	Q_{2_2}	24	59	31
	Q_{4_1}	−72	−87	−62
^{102}Ru	$E_{10_1^+}$	3.494	3.856	
	$B(0_2^+\to 2_2^+)$	3868	1425	
	$B(4_1^+\to 2_2^+)$	54	94	
	$B(2_3^+\to 0_1^+)$	3	0	13
	$B(3_1^+\to 4_1^+)$	687	357	
	$B(3_1^+\to 2_2^+)$	1839	741	
	$B(3_1^+\to 2_1^+)$	60	44	
	Q_{2_2}	31	49	38
	Q_{4_1}	−71	−67	−69
^{104}Ru	$B(0_2^+\to 2_2^+)$	5606	745	
	$B(4_1^+\to 2_2^+)$	122	47	
	$B(3_1^+\to 4_1^+)$	684	212	
	$B(3_1^+\to 2_2^+)$	2072	655	
	$B(3_1^+\to 2_1^+)$	66	99	
	Q_{2_2}	27	46	60
	Q_{4_1}	−82	−49	−90
^{100}Pd	$E_{4_2^+}$	2.356	2.113	
	$E_{5_1^+}$	3.260	2.866	
	$E_{6_2^+}$	3.226	2.904	
	$E_{0_3^+}$	2.721	2.050	
	$E_{0_2^+}$	1.148	1.367	
	$E_{2_3^+}$	2.167	2.096	

(*Continue*)

1	2	3	4	5
^{102}Pd	$E_{5_1^+}$	2.757	3.218	
	$E_{6_2^+}$	2.831	3.153	
	$E_{0_3^+}$	1.872	2.336	
	$B(4_1^+\to 2_2^+)$	61	198	
	$B(3_1^+\to 4_1^+)$	315	641	200
	$B(3_1^+\to 2_2^+)$	916	498	
	$B(3_1^+\to 2_1^+)$	96	0	94
	Q_{2_2}	19	57	36
	Q_{4_1}	−57	−97	−71
^{104}Pd	$E_{6_2^+}$	2.842	3.125	
	$B(0_2^+\to 2_2^+)$	878	2530	
	$B(4_1^+\to 2_2^+)$	25	165	
	$B(3_1^+\to 4_1^+)$	447	584	340
	$B(3_1^+\to 2_2^+)$	1226	814	
	$B(3_1^+\to 2_1^+)$		16	
	Q_{2_2}	19	59	37
	Q_{4_1}	−46	−89	−71
^{106}Pd	$E_{6_2^+}$	2.609	2.815	
	$B(2_3^+\to 0_1^+)$	54	0	7
	$B(3_1^+\to 4_1^+)$	538	274	780
	$B(3_1^+\to 2_2^+)$	1606	1378	
	$B(3_1^+\to 2_1^+)$	40	68	
	$B(4_1^+\to 2_2^+)$	120	67	
	Q_{2_2}	23	48	40
	Q_{4_1}	−76	−58	−74
^{108}Pd	$E_{10_1^+}$	3.282	3.691	
	$E_{8_1^+}$	2.457	2.660	
	$E_{5_1^+}$	2.109	2.342	
	$E_{6_2^+}$	2.208	2.433	

(*Continue*)

1	2	3	4	5
^{108}Pd	$B(3_1^+ \to 4_1^+)$	952	1037	520
	$B(3_1^+ \to 2_2^+)$	2379	1876	
	$B(3_1^+ \to 2_1^+)$	50	0.2	
	$B(4_1^+ \to 2_2^+)$	182	358	
	Q_{2_2}	17	41	57
	Q_{4_1}	−80	−116	−83
^{110}Pd	$E_{5_1^+}$	1.898	2.059	
	$B(4_1^+ \to 2_2^+)$	180	31	
	$B(3_1^+ \to 4_1^+)$	940	55	510
	$B(3_1^+ \to 2_2^+)$	2351	2181	
	$B(3_1^+ \to 2_1^+)$	33	45	
	Q_{2_2}	20	9	62
	Q_{4_1}	−79	−30	−95
^{112}Pd	$E_{8_1^+}$	2.218	2.341	
	$E_{10_1^+}$	3.020	3.300	
	$E_{4_2^+}$	1.360	1.318	
	$E_{5_1^+}$	1.936	1.933	
	$E_{6_2^+}$	2.017	2.050	
	$E_{0_3^+}$	1.226	1.124	
	$E_{2_3^+}$	1.625	1.533	

a) The level energies in the Yrast-region of both chains of isotopes are excellently reproduced by the AVM up to spin 10 (and even higher for some cases) thus confirming the assumption for their collective nature, while IBM-versions are unable to reproduce exactly the energies of states higher then 6 in several isotopes.

b) For the side-bands, the level energy are well reproduced by the AVM. Except the rare cases, where the discrepancies achieve 0.2—0.3 MeV, they are generally of order 0.1 MeV or even smaller. Note that the energies of «three-phonon» states with spin 0 and 3 are described remarkable good in contrary to the IBM-versions.

c) The β-band levels, 0_2^+ and 2_3^+ are suprisingly good described by the AVM, while both the IBM-1 and IBM-2 fail to reproduce their energies.It might be considered also as «rehabilitation» of the collective status of those levels.

d) Concerning the energies, the most interesting results are obtained for ^{104}Ru and ^{110}Pd, where the complete correspondence could be established between all the known experimental levels of positive parity and the theoretical ones up to energy $E=3.5-4$. MeV. The main E2-properties of these nuclei are described by the model remarkably good too.

e) The enhanced E2-transition probabilities, $(\Delta N=1)$, are successfully described by the AVM as well as the IBM, for the experimental errors being still relatively big. Note the extremely good AVM-description of the data set on quantities $B(\mathrm{E2};\ 0_2 \to 2_1)$ which it is commonly difficult to reproduce.

f) The AVM appears able to describe the enhanced transition probabilities inside the two-phonon triplet, namely, $B(\mathrm{E2};\ 0_2 \to 2_2)$, whereever such information is available.

g) The probabilities of hindered E2-transitions (crossover) are described satisfactorily by the AVM as well as IBM.

i) For the inside Yrast-band transitions, the dependence of their probabilities on the spin is reproduced by the AVM remarkable good for the cases where experimental information exists.

Thus, we have succeeded in reproducing systematically the collective features of typical soft spherical nuclei, Pd and Ru, which was achieved by using a very limited number of parameters.

One should note the improving quality of AVM-results going up in the energy scale (see Figs 1, 2, 9—11) in contrast to the various IBM-versions. One could interpret it as follows. The nuclei under consideration are soft enough to manifest large-amplitude quadrupole mean field oscillations to which the single-particle level scheme is very sensitive. Thus the resulting collective potential energy $U(\beta)$ versus the collective deformation parameter β feels fluctuations near the zero point and its approximation by the formula (1) isn't very good. Going to the higher energy (and angular momentum), one has a deep potential well, for which the approximation (1) is well enough to compute the level energies determined by the large-β asymptotic only and slightly influenced by the potential energy fluctuations at small β.

From the results of the work the following conclusions might be drawn.

(i) The model considered in present paper proves to be very successful in describing collective quadrupole excitations in soft spherical nuclei providing the agreement with the experiment not worse then the famous IBM, while the number of parameters fitted

being not greater than that of IBM-versions. Thus an extension of such AVM-calculations to other regions of periodical table seems to be of interest.

(ii) The values of parameters optimized to fit the physical quantities are in accordance with the initial microscopic estimations thus making the whole approach to seem selfconsistent and stimulating the work to construct the collective Hamiltonian and calculate its coefficients by means of the straightforward microscopic computations basing on the underlying fermionic dynamics.

Aknowledgement

The author is extremely grateful to Prof. Zelevinsky for many helpful discussions, a current interest to the work and for the help in preparing the manuscript. He thank also Drs V.F. Dmitriev and P.N. Isaev for their kindly helping in beginning of the work with the computer system.

REFERENCES

1. *A. Bohr and B. Mottelson.* Nuclear Structure, t2, M., Mir, 1977.
2. *A. Arima and F. Iachello.* Ann. Phys. N. Y. 1976, 99, 253.
3. *A. E. L. Dieperink and R. Bijker.* Phys. Lett. 1982, 116B, 77.
4. *V. G. Zelevinsky.* Materials of the XVI Winter School LINP, L., 1981, p.121.
5. *K. Summerer.* Nucl. Phys. 1980, A339, 74.
6. *R. V. Jolos et al.* PEPAN 1985, 16, 280.
7. *P. Van Isacker et al.* Nucl. Phys. 1982, A380, 383.
8. *V. G. Zelevinsky.* Sov. Phys. Izvestia. ser. Fys. 1985, 49, 1.
9. *P. Van Isacker.* Interacting Bose-Fermi Systems in Nuclei,
F. Iachello ed., Plenum Press, N. Y., 1981, 59.
10. *S. G. Lie and G. Holzwarth.* Phys. Rev. 1985, C12, 1035.
11. *F. K. McGowan et al.* Nucl. Phys. 1968, A113, 529.
12. *E. H. Du Marschie et al.* Nucl. Phys. 1981, A355, 93.
13. *W. F. Piel et al.* Phys. Rev. 1981, C23, 708.
14. *K. Summerer et al.* Nucl. Phys. 1978, A308, 1.
15. *O. K. Vorov and V. G. Zelevinsky.* Yad. Fyz. 1983, 37, 1392.
16. *O. K. Vorov and V. G. Zelevinsky.* Nucl. Phys. 1985, A439, 207.
17. *J. Stachel et al.* Nucl. Phys. 1984, A419, 589.
18. *J. Stachel et al.* Nucl. Phys. 1982, A383, 429.
19. *P. J. Tivin et al.* J. Phys. G 1977, 9, 1267.
20. *W. Andreitscheff et al.* Nucl. Phys. 1986, A448, 301.
21. *H. H. Bolotin, A. E. Stuchbery et al.* Nucl. Phys. 1981, A370, 146.
22. *T. Kishimoto and T. Tamura.* Nucl. Phys. 1976, A270, 317.
23. *T. Kishimoto and T. Tamura.* Nucl. Phys. 1972, A192, 246.
24. *P. M. Endt.* Nucl. Data Tables 1981, 26, 48.
25. *M. Sambataro.* Nucl. Phys. 1982, A380, 365.
26. *P. Van Isacker and G. Puddu.* Nucl. Phys. 1980, A348, 125.

27. *O. K. Vorov and V. G. Zelevinsky.* Proc. of the Seminar «Group Theory Methods in Physics», Rijga, 1985 ; Preprint INP-85-120.
28. *L. Hasselgren and D. Cline.* Interacting Bose—Fermi Systems in Nuclei,
F. Iachello, ed., Plenum Press, N. Y., 1981, 59.
29. *R. V. Jolos et al.* Sov. PEPAN, 1985, 16, N2, 280.
30. *U. Kaup, A. Gelberg.* Z. Phys. 1979, A293, 311.
31. *Ju. Ju. Zykov and G. I. Sychikov.* Preprint 11-83, Nuclear Physics Institute, Alma-Ata (1983).
32. *Ju. Ju. Zykov and G. I. Sychikov.* Preprint 4-84, Nuclear Physics Institute, Alma-Ata (1984).
33. *K. Weeks and T. Tamura.* Phys. Rev. 1980, C22, 888.
34. *S. Landsberger et al.* Phys. Rev. 1980, C21, 588.
35. *E. E. Berlovich, S. S. Vasilenko and Ju. N. Novikov* «Lifetimes of Nuclear States», M., «Nauka», 1972.
36. *V. V. Babenko et al.* Sov. Phys. Izvestia Ser. Fyz. 1978, 42, 93.
37. *M. Sakai. Nucl.* Data Tables 1984, 31, 399.
38. *J. A. Grau et al.* Phys. Rev. 1976, C14, 2297.
39. *I. Y. Lee et al.* Phys. Rev. 1982, C25, 1865.
40. *R. L. Robinson et al.* Nucl. Phys. 1969, A124, 553.
41. *M. Luontama et al.* Jyvaskyla, 1985, Preprint JYFL 12/85.
42. *G. A. Shevelev.* Thesises to XXXII Conf. on Nucl. Spectroscopy and Nuclear Structure, 1982, Leningrad, 72.
43. *B. E. Stepanov.* Yad. Fys. 1973, 18, 99.
44. *J. Lande et al.* Nucl. Phys. 1977, A292, 301.
45. *R. V. Jolos et al.* Thesises to XXV Conference on Nucl. Spectroscopy and Nuclear Structure, Leningrad, 1975, p.200.
46. *O. K. Vorov and V. G. Zelevinsky.* Sov. Phys. Isvestia ser. Fyz. 1987.
47. *A. Passoja et al.* Jyvaskyla, 1985, Preprint JYFL 1/85.
48. *A. Zemel et al.* Phys. Rev. 1985, C31, 1483.
49. *K. Heyde et al.* Nucl. Phys. 1983, A398, 235.
50. *O. K. Vorov.* 1986, Preperint INP-86-86, Novosibirsk.
51. *O. K. Vorov.* Novosibirsk, Program Package «NINA», 1986.
52. *J. Stachel et al.* Phys. Rev. 1982, C25, 650.
53. *G. Winter et al.* J. of Phys. 1985, G11, 277.
54. *E. Maglione.* Interacting Bose-Fermi Systems in Nuclei,
F. Iachello ed., Plenum Press, N. Y., 1981, p.217.

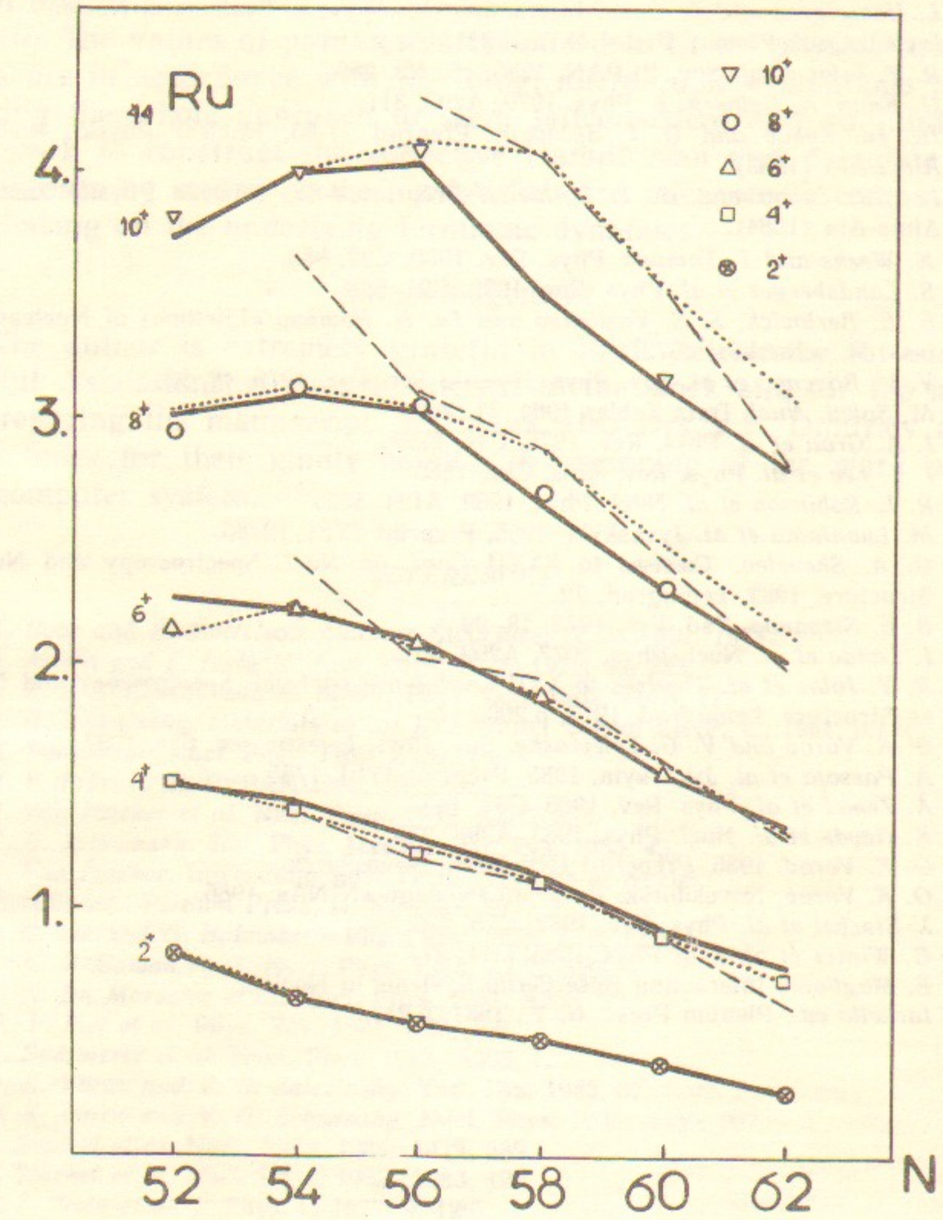

Fig. 1. Energy levels of the Yrast-band in even Ru isotopes empirical (circles) and calculated in the AVM (solid line), IBM-2 (dashed line) and IBM-1 (dotted line) versus the neutron number. The experimental values are taken mostly from the last version of Sakai Tables [37].

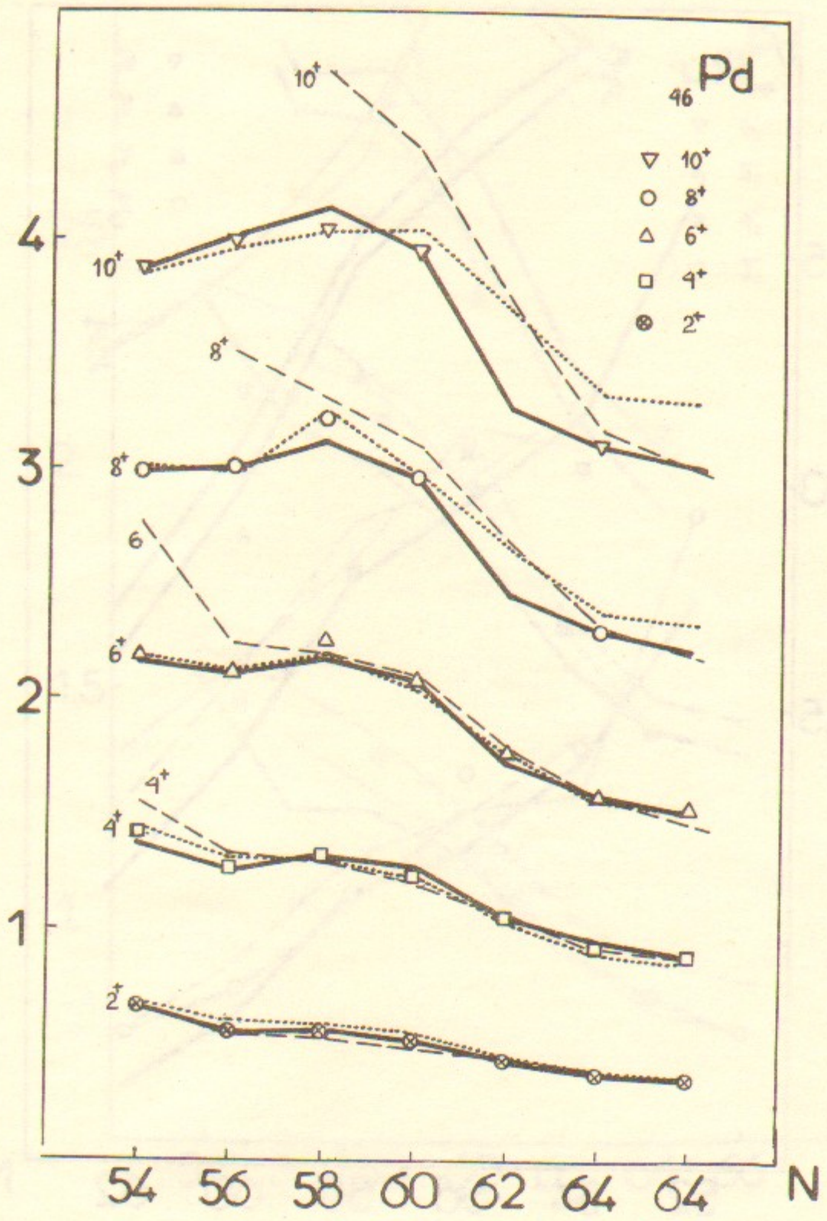

Fig. 2. The same as in Fig. 1, but for even Pd isotopes. Experimental data are taken mostly from [37].

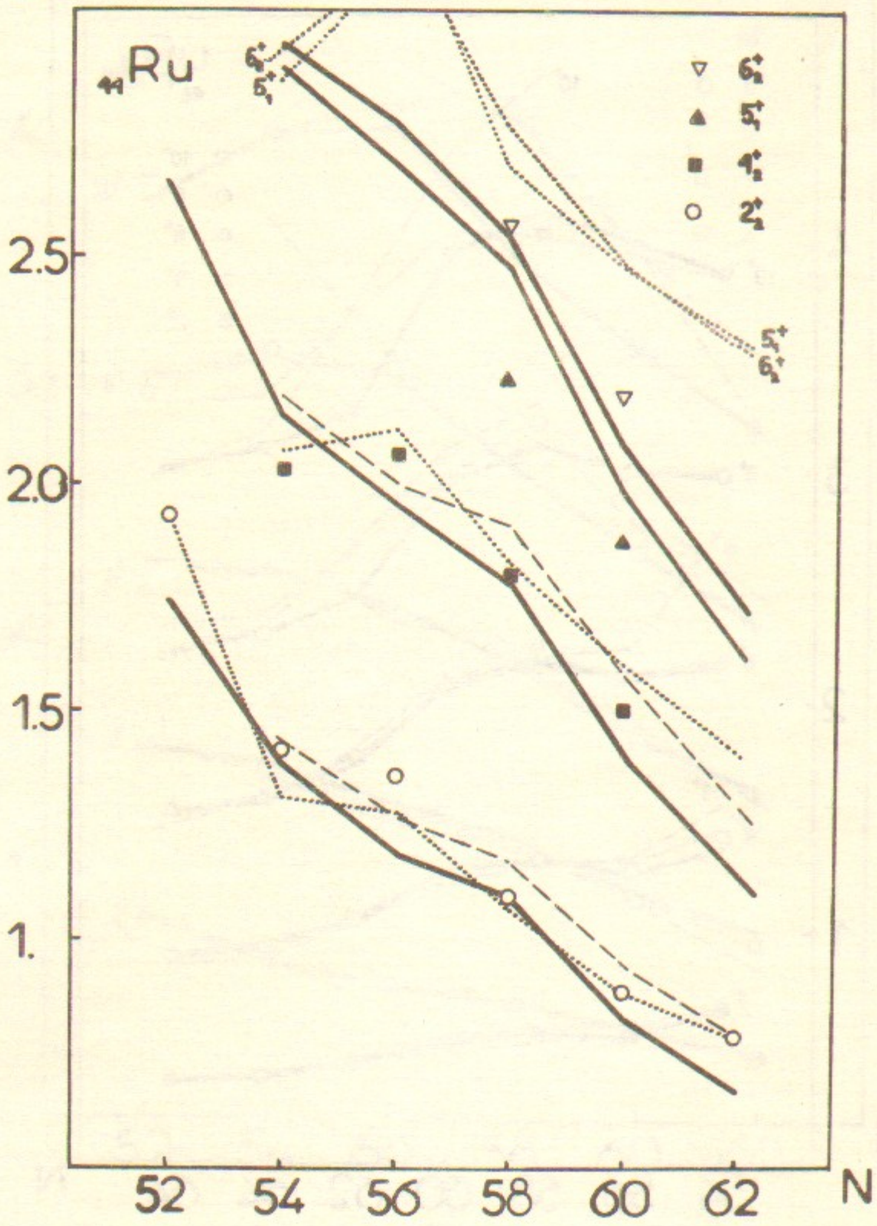

Fig. 3. Energies of the *X*-band levels and of the level 5_1^+ (*Z*-band)—empirical (circles) and calculated in the AVM (solid line), IBM-2 (dashed line) and IBM-1 (dotted line).

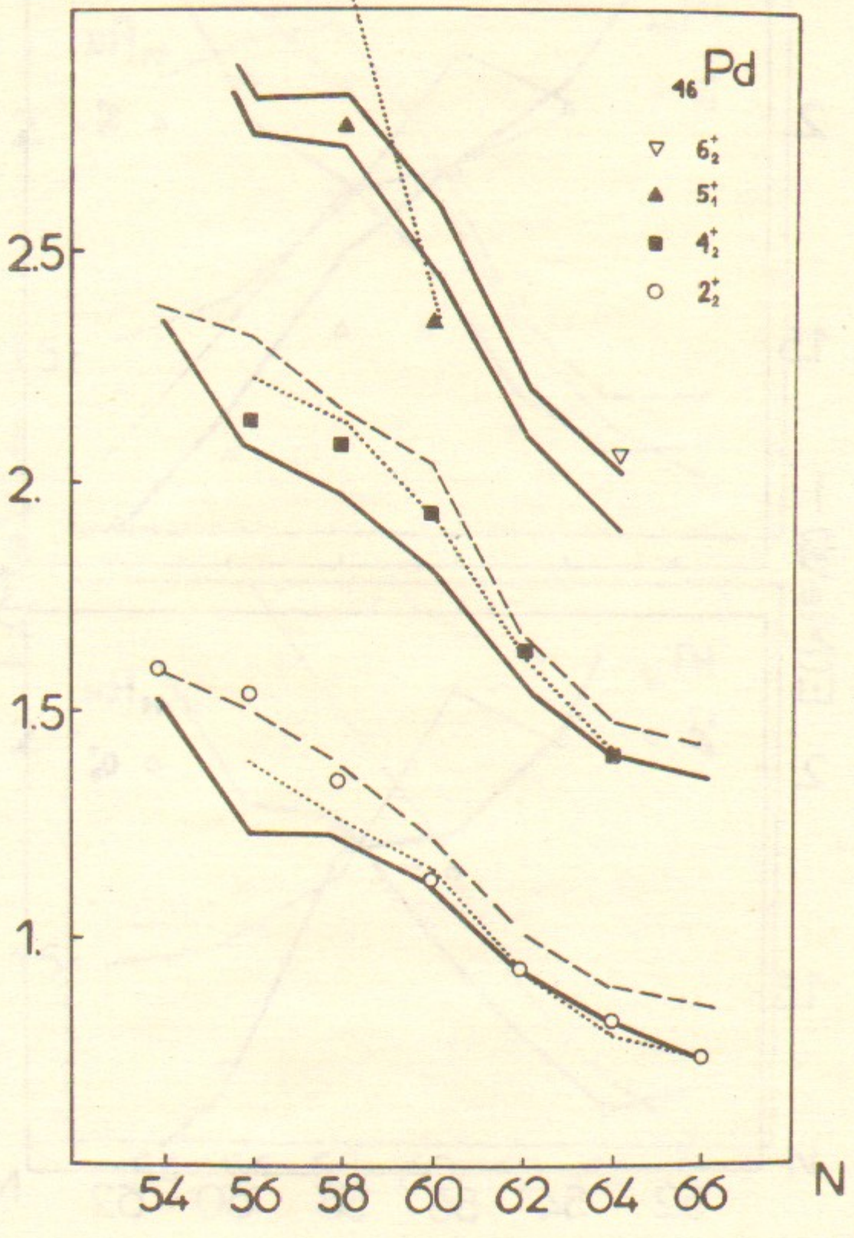

Fig. 4. The same as in Fig. 3 but for Pd isotopes.

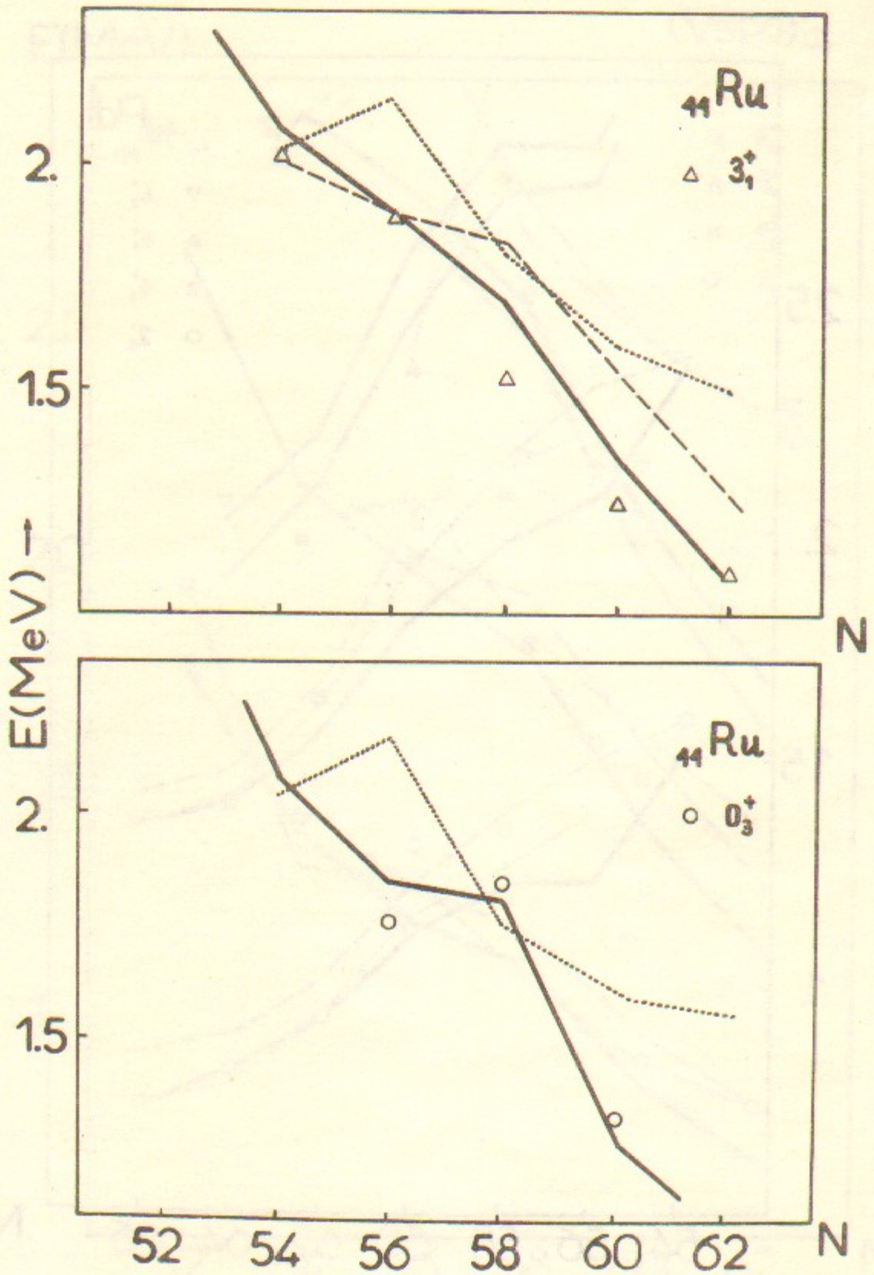

Fig. 5. The energies of three-phonon states 3_1^+ (upper part) and 0_3^+ (lower one) for Ru isotopes. AVM-results are given by the solid line, those for IBM-2 and IBM-1 are given by the dashed line and dotted one respectively.

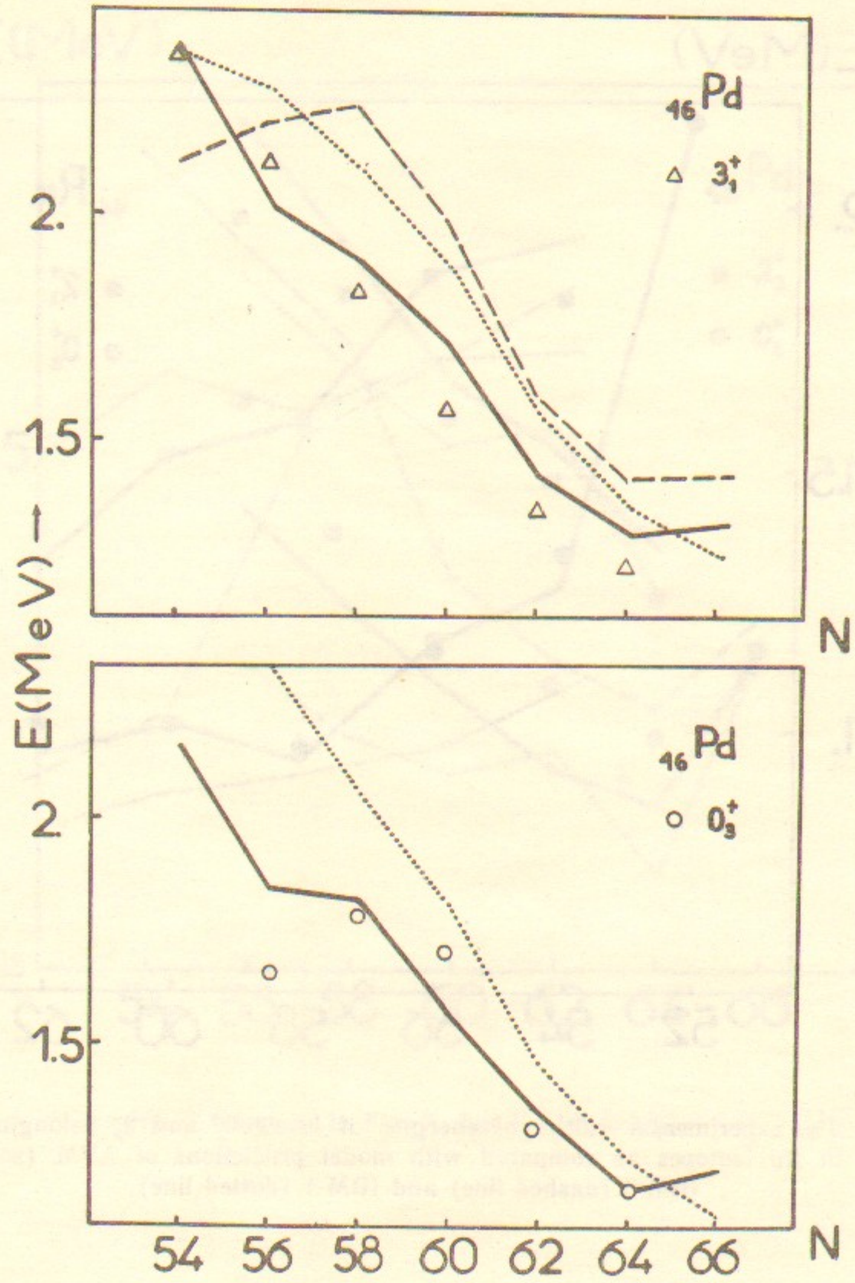

Fig. 6. Same as in Fig. 5, but for Pd isotopes.

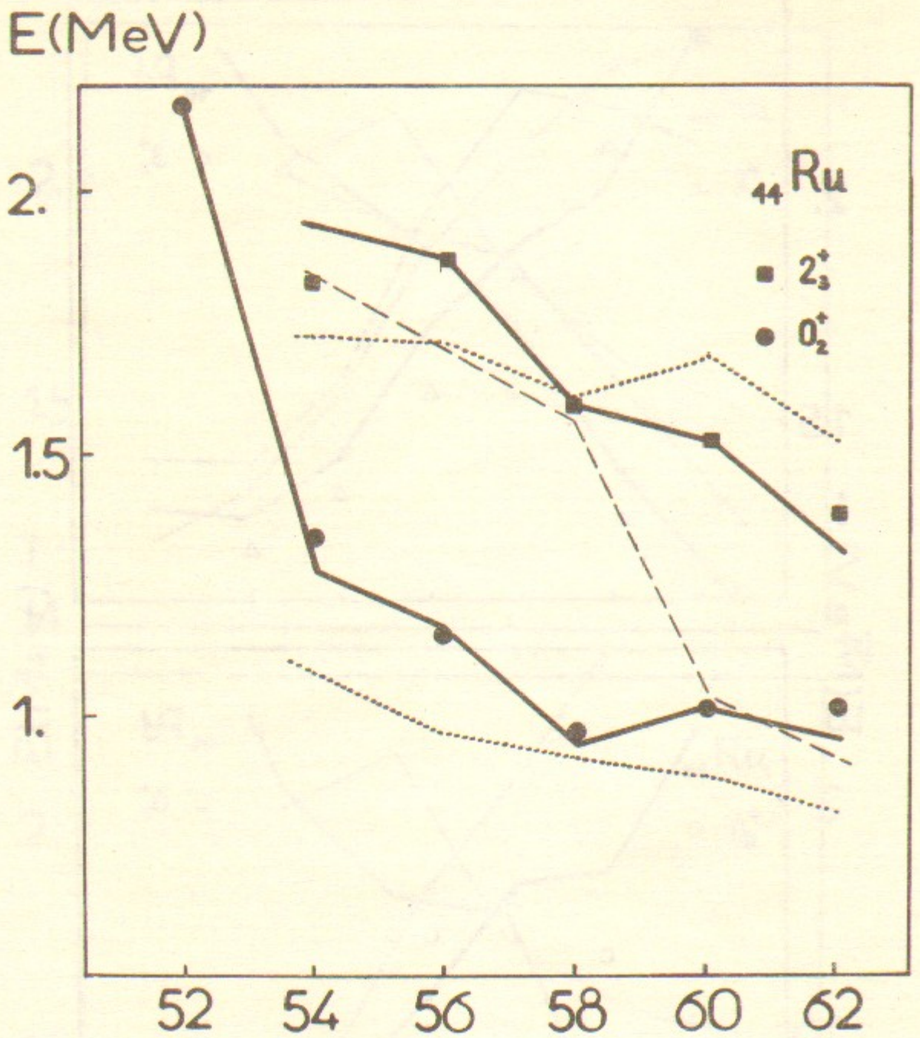

Fig. 7. The experimental values of energies of levels 0_2^+ and 2_3^+ belonging to the β-band in Ru isotopes as compared with model predictions of AVM (solid line), IBM-2 (dashed line) and IBM-1 (dotted line).

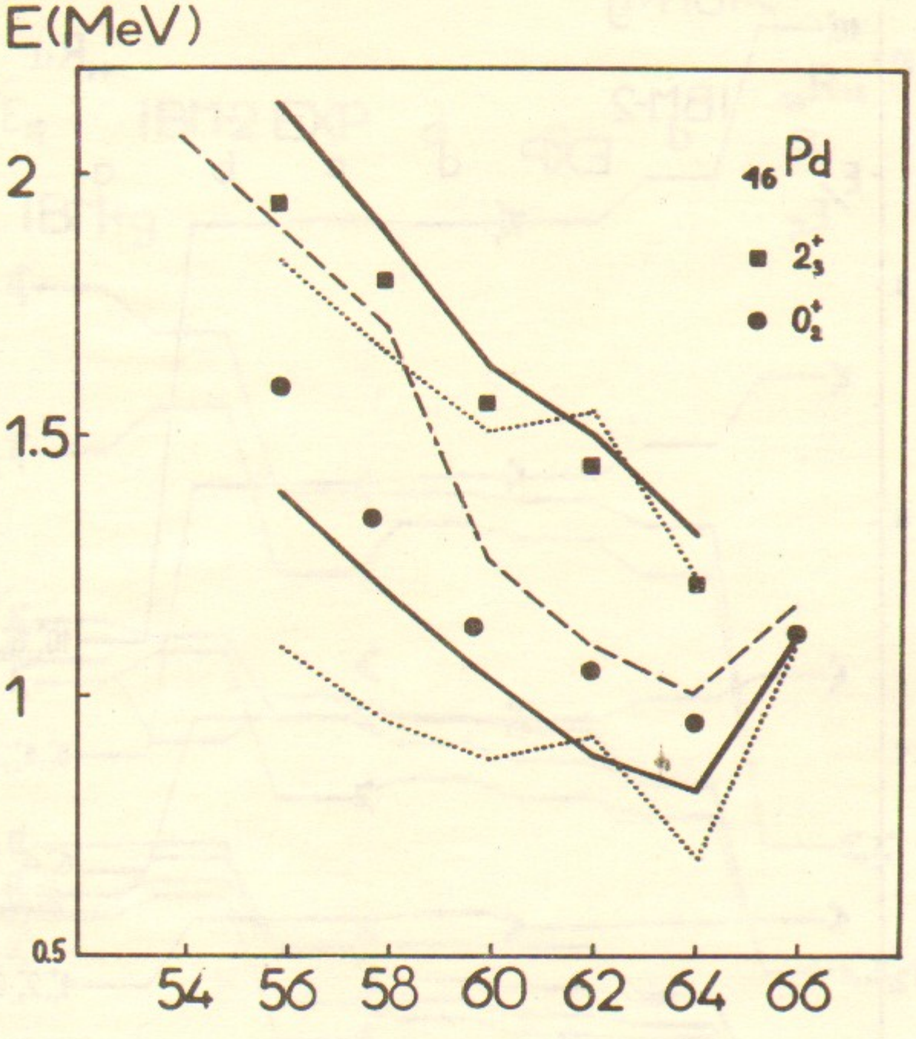

Fig. 8. Same as in Fig. 7., but for Pd isotopes.

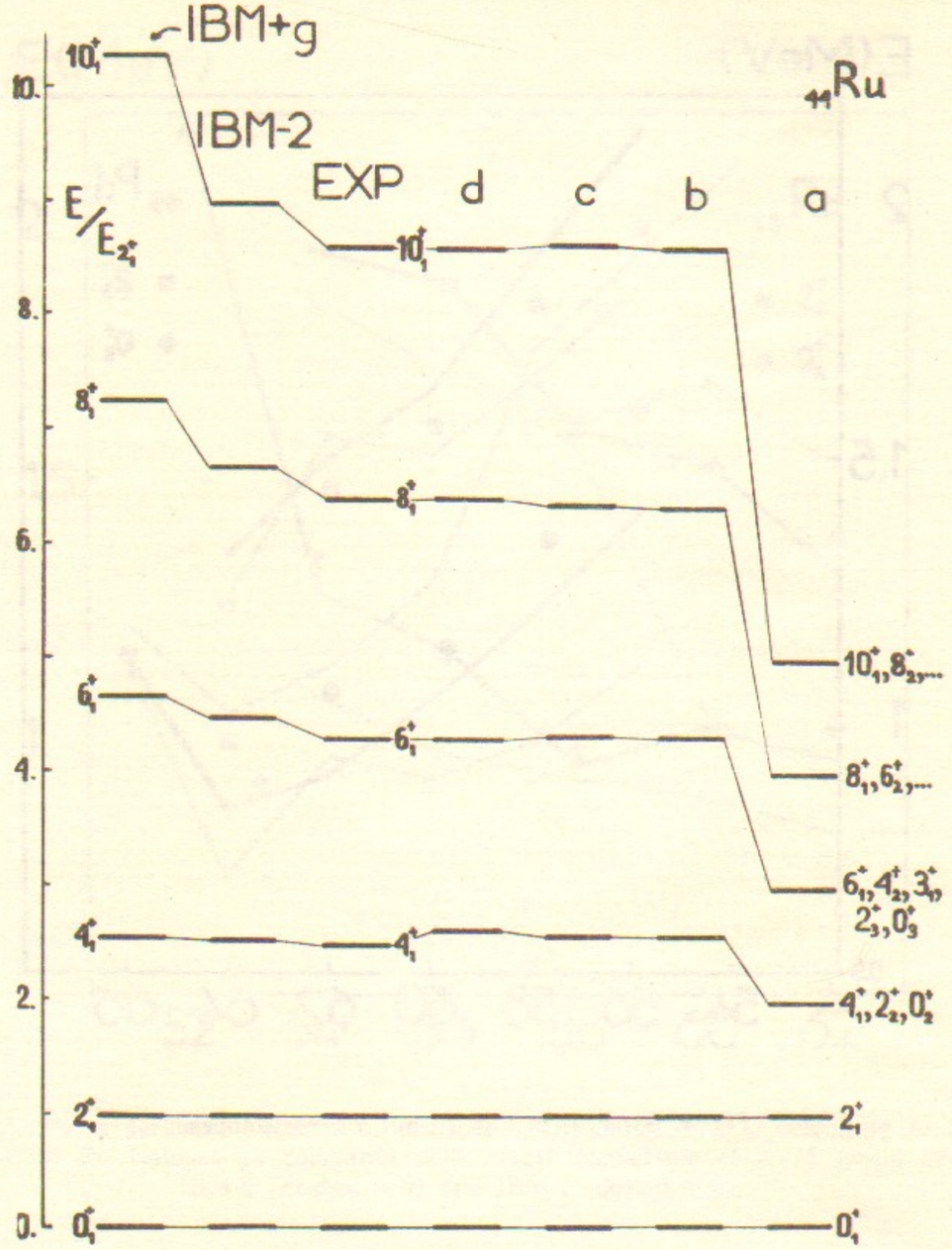

Fig. 9. Level energies of the Yrast-band in Ru isotepes (Ref. [17, 18], middle part) as compared with those calculated in AVM (on the right). Labels *a*, *b*, *c*, *d* correspond to the following approximations:

a—pure harmonic vibrator, *b*—«quartic asimptotics», (for $\mathring{\omega}^2=0$ and one more parameter $\sigma>0$ being used), *c*—results for parameter $\mathring{\omega}^2/\lambda^{2/3}$ being fitted, *d*—the full calculational scheme (for three parameters $\mathring{\omega}^2/\lambda^{2/3}$, χ, σ being fitted). The IBM-2 calculations and those for IBM+g [17, 18, 49] are also given for comparison on the left).

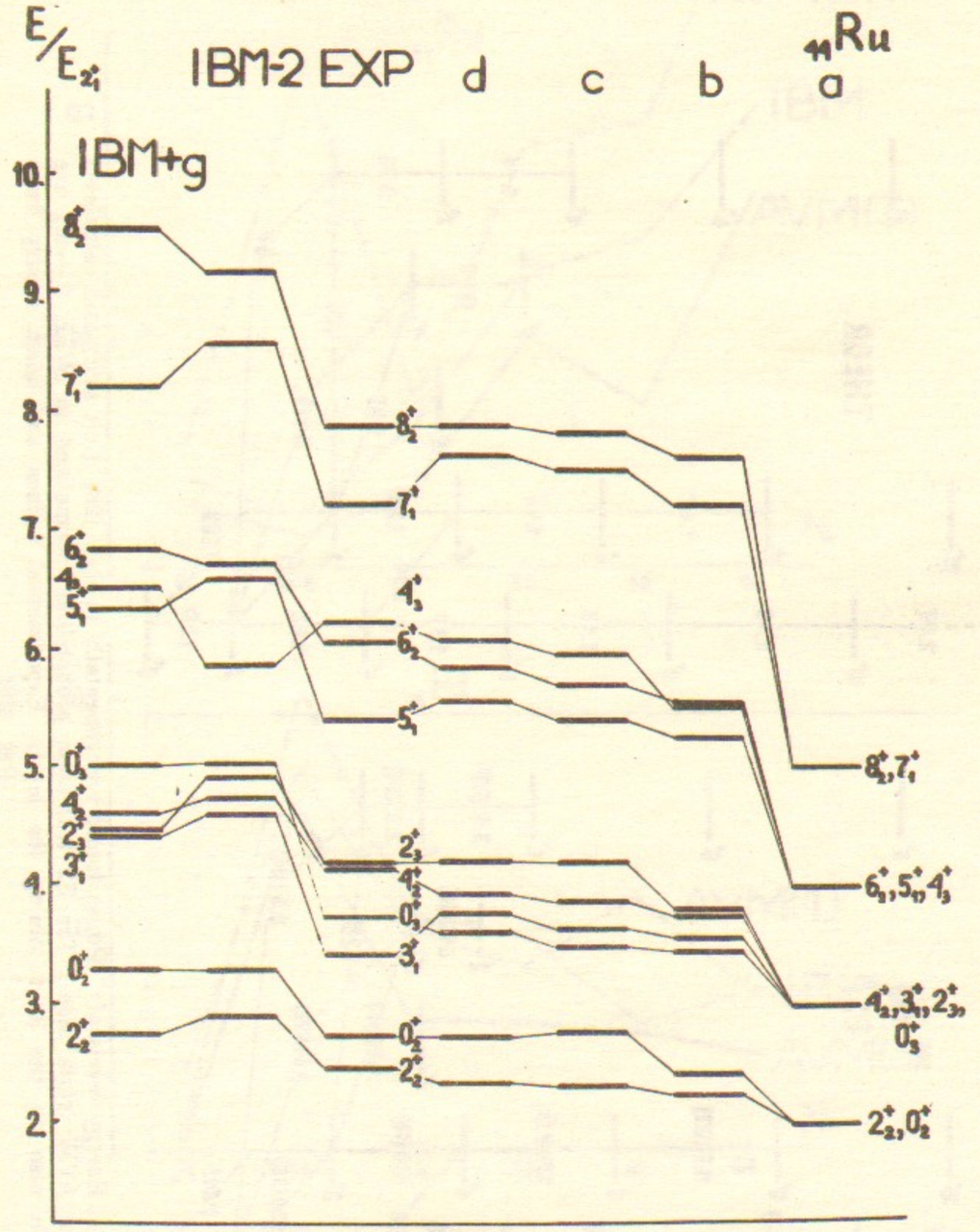

Fig.10. Same as in Fig. 9., but for side bands in Ru.

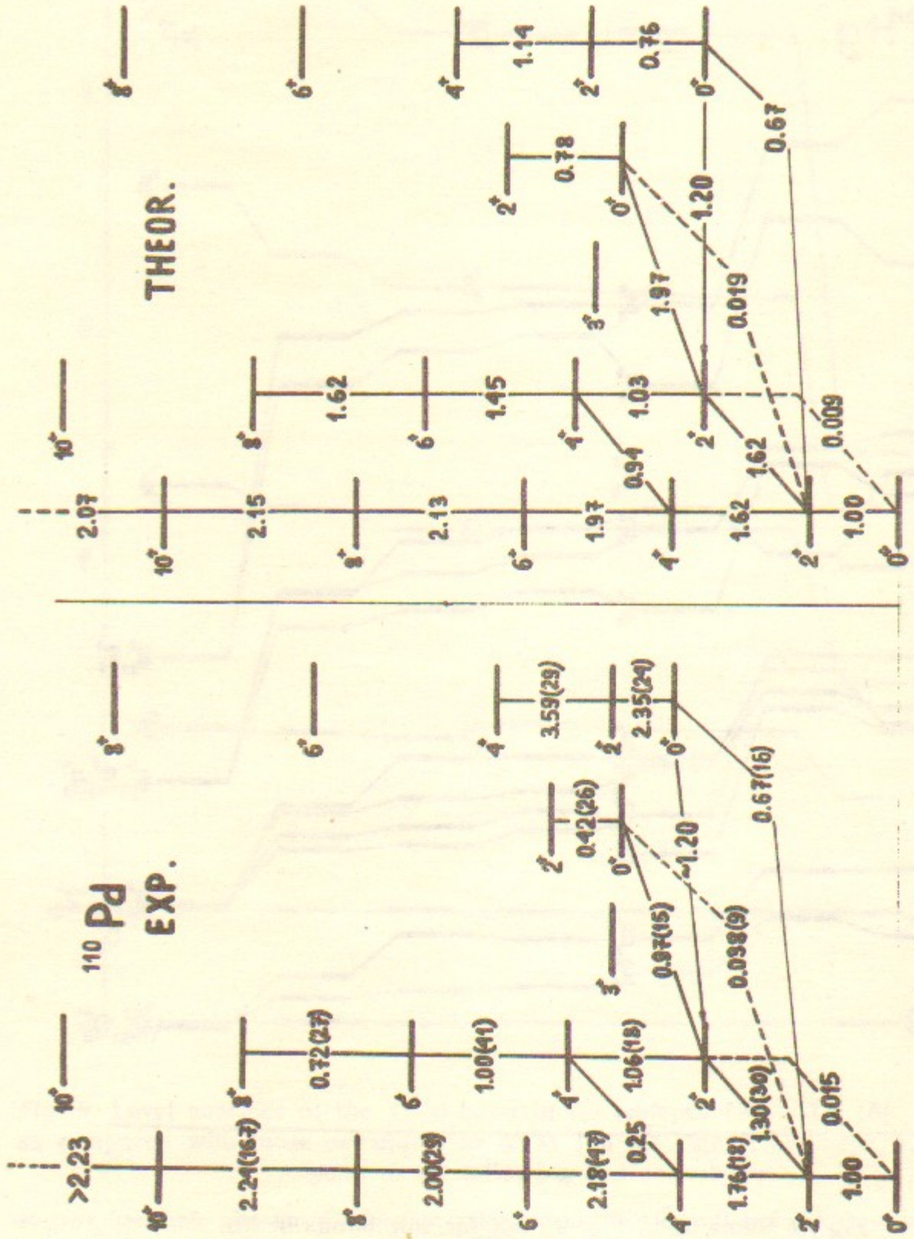

Fig.11. Energy levels of ^{110}Pd as found experimentally in Ref. [28] (left side) and calculated in the AVM (right side). The E2 transition probabilities normalized to $B(E2; 2_1 \rightarrow 0_1)$ are shown also on the lines joining the levels. Experimental values are taken mostly from Ref. [28].

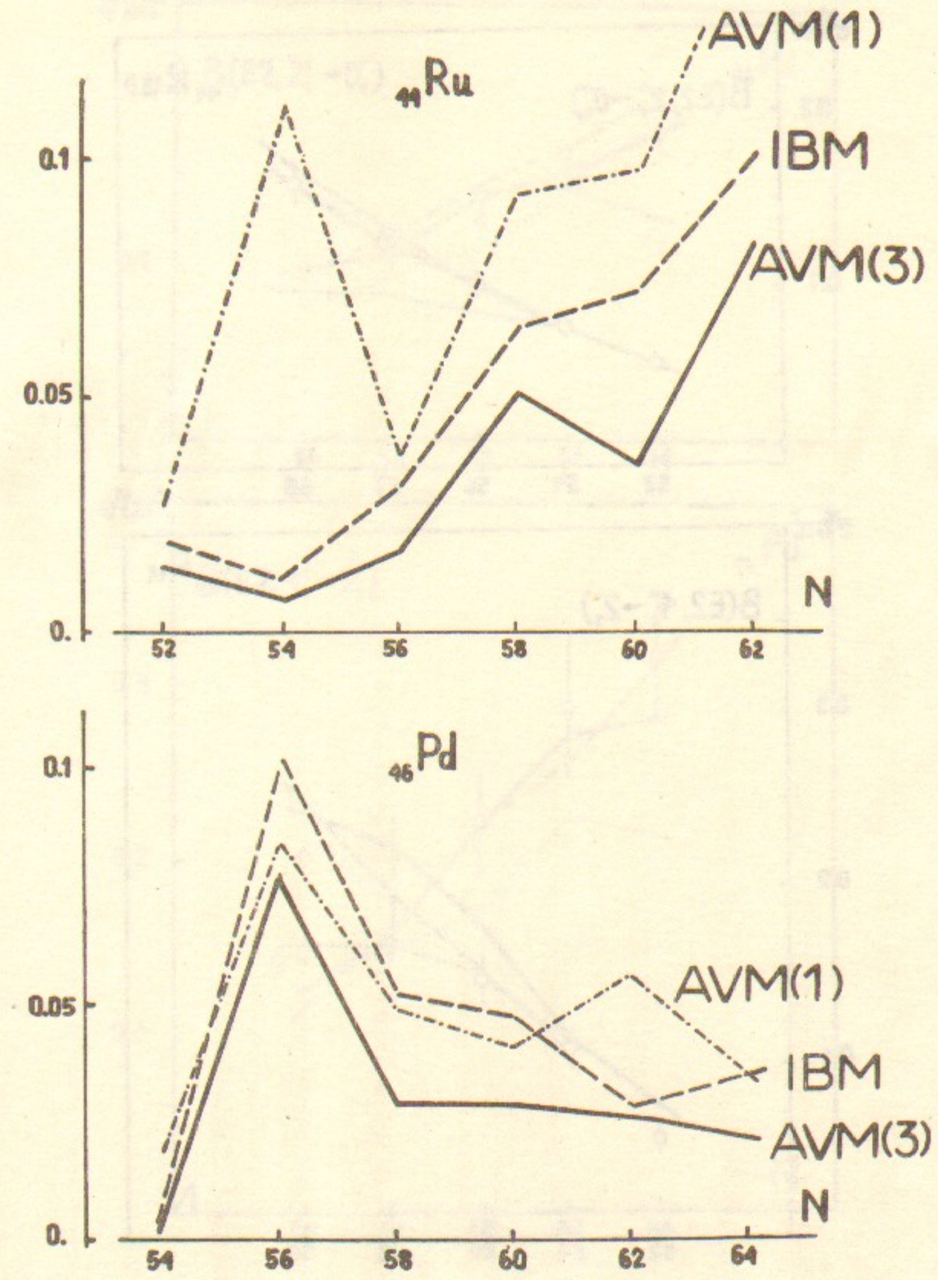

Fig.12. *a*—The averaged squared deviations of experimental level energies (normalized to $E_{2_1^+}$) in Ru isotopes from calculated in IBM-1 (SU(5) limit), dashed line, and in the AVM for only one fitted parameter, σ, (dotted line) and for all three dynamical parameter being fitted. The number of fitted parameter is shown in brackets for each case. *b*—The same as in Fig. 12,*a* but for Pd isotopes.

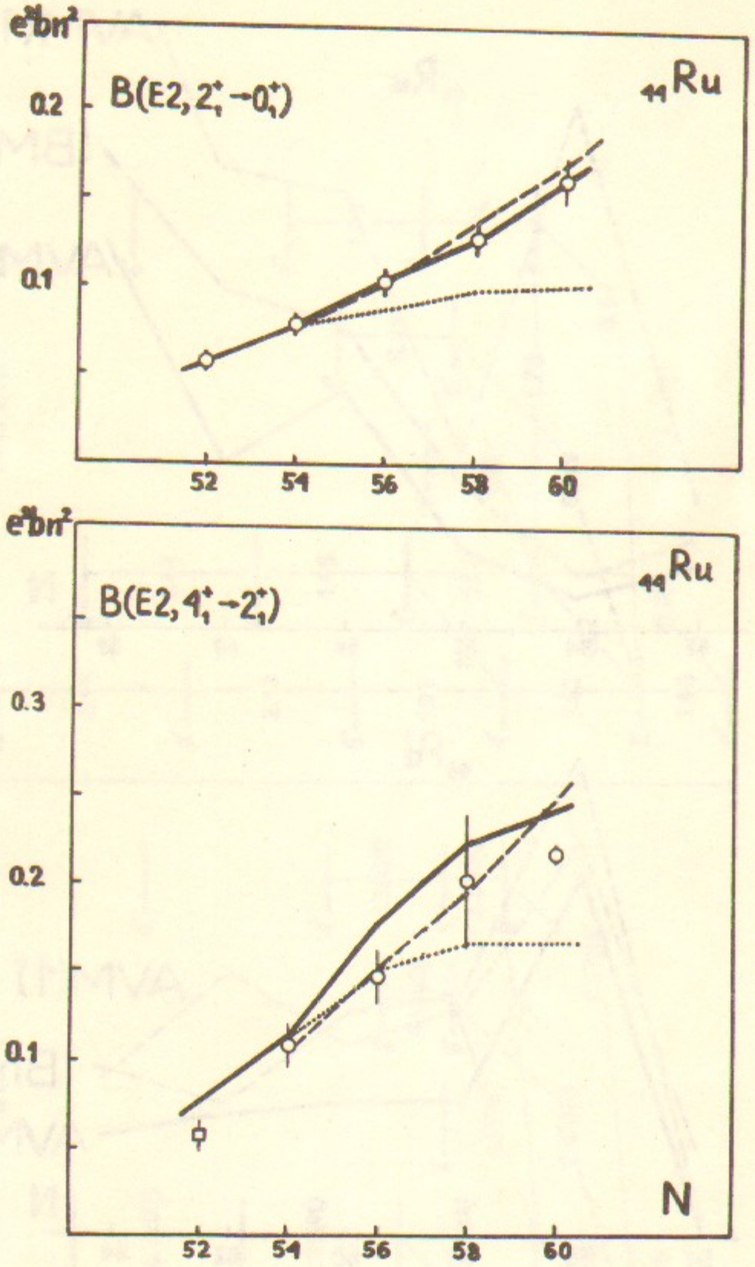

Fig.13. *a*—The absolute values of $B(E2; 2_1^+ \to 0_1^+)$ for the chain of Ru isotopes Ru as compared with AVM-results (solid line) and those for IBM-2 (dashed line) and IBM-1 (dotted line). Experimental data are taken from Ref. [33]. *b*—Same as in part *a* but for $B(E2; 4_1^+ \to 2_1^+)$-values. Experimental data are taken: circles from [33], squares from [34].

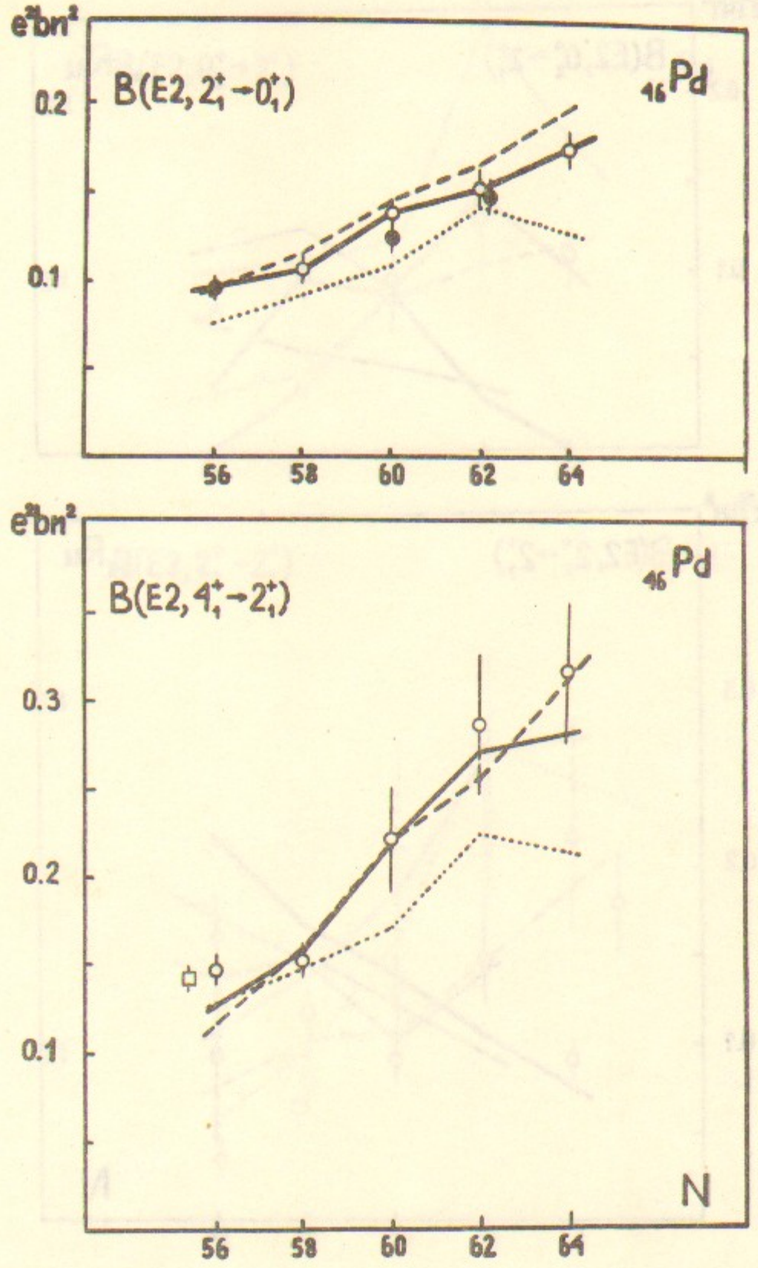

Fig.14. *a*—Same as in Fig. 11*a* but for the chain of Pd isotopes. Experimental data are taken: opened circles from [35], closed circles from [33]. *b*—Same as in Fig. 11, part *a* but for Pd isotopes. Experimental data are taken: circles from [33], squares from [41].

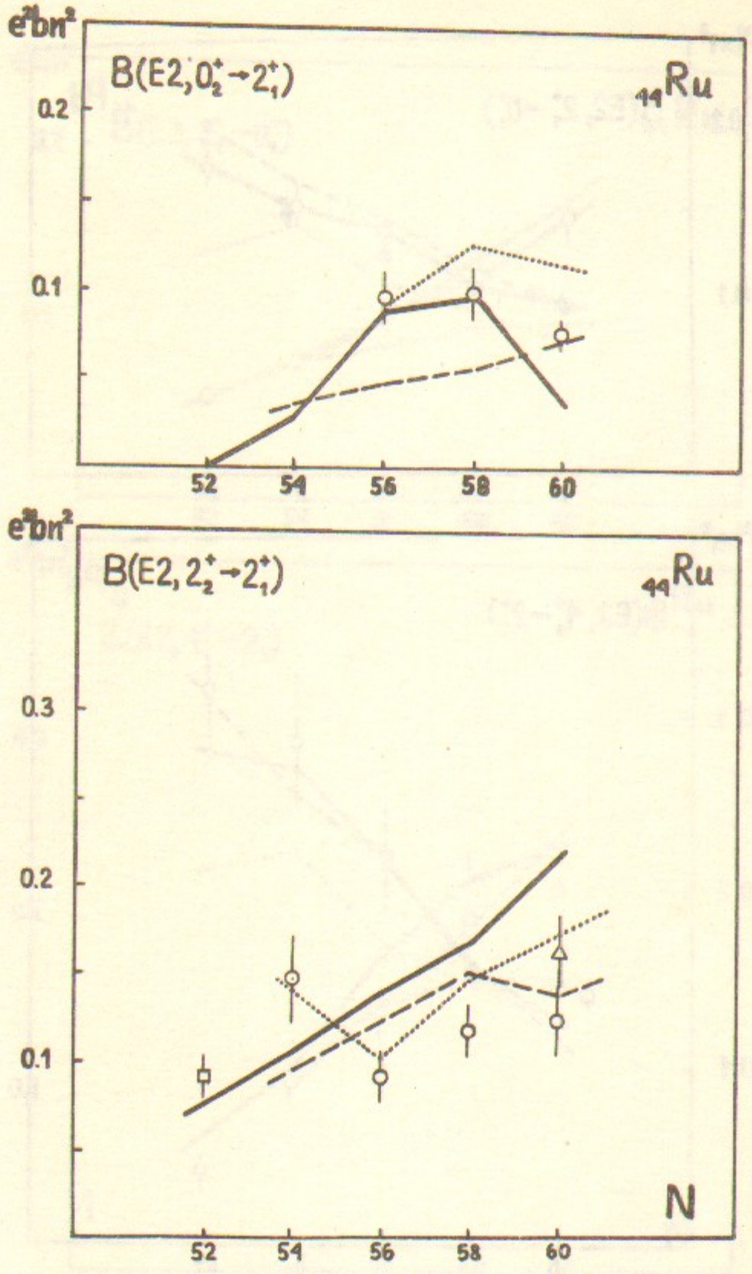

Fig. 15. a—Absolute values of B(E2; $0_2^+ \to 2_1^+$) in Ru isotopes and results of calculations in IBM-2 (Ref. [26], dashed line), IBM-1 (Ref. [32], dotted line), and in the AVM (solid line). Experimental values are taken from Ref. [33]. *b*—The same as in the part *a* but for B(E2; $2_2^+ \to 2_1^+$). Experimental values are taken: circles from [33], squares and triangles from [34].

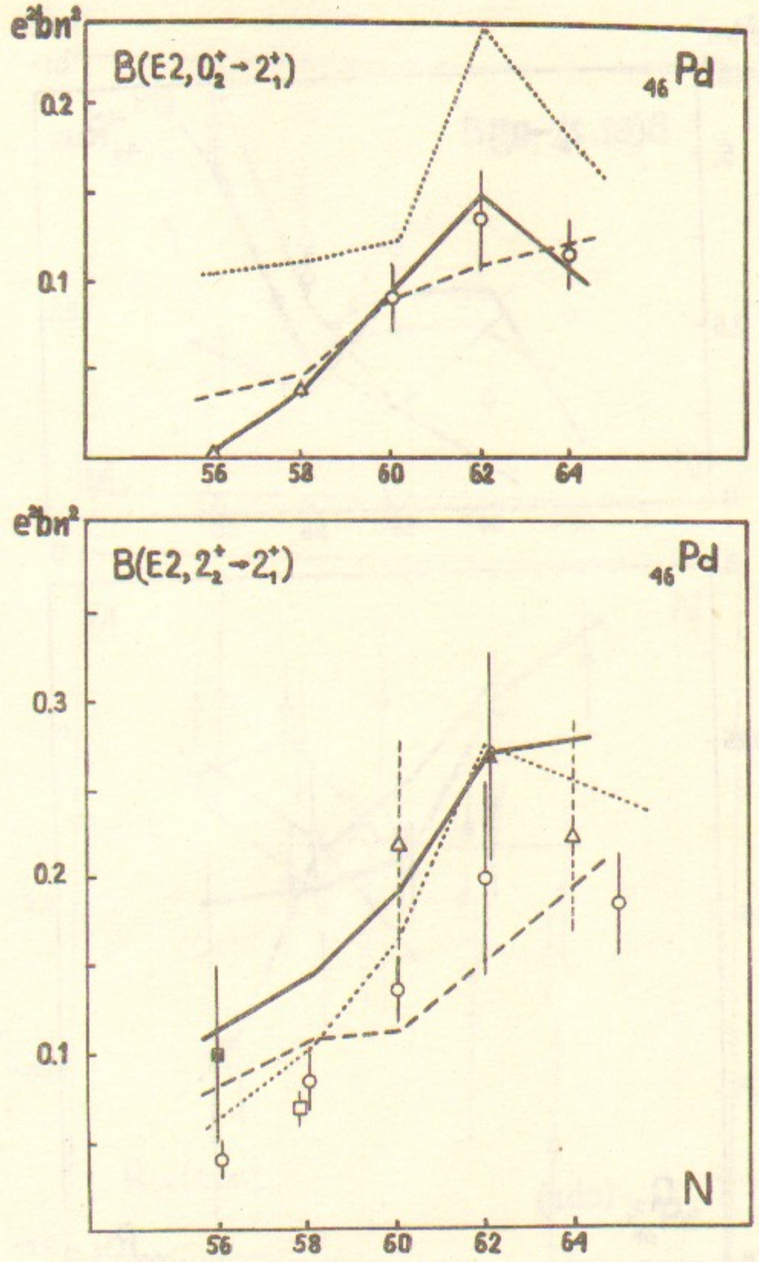

Fig. 16. a—Absolute values of B(E2; $0_2^+ \to 2_1^+$) for Pd isotopes and results of calculations in IBM-2 (Ref. [26], dashed line), IBM-1 (Ref. [32] *), dotted line), and in the AVM (solid line). Experimental values are taken: circles from [33], triangles from [41]. *b*—The same as in part *a* but for B(E2; $2_2^+ \to 2_1^+$). The experimental data are taken: circles from [33], opened triangles from [43], closed triangles from [40], closed squares from [44], opened squares from [41].

*) Since the numerical values for this quantity obtained in Ref. [32] are wrong those are corrected by the present author.

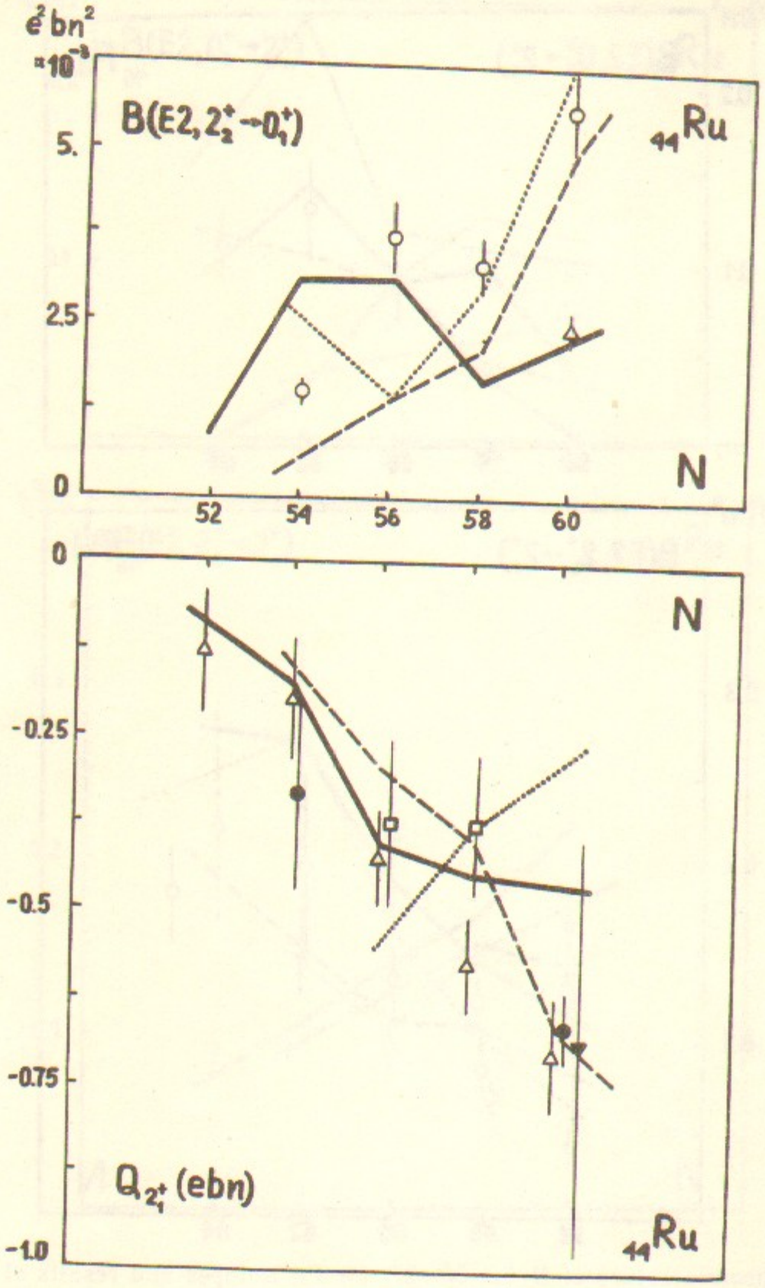

Fig. 17. a—Absolute values of the crossover transition probabilities, $B(E2; 2_2^+ \to 0_1^+)$ in Ru isotopes compared with those callculated in IBM-2 (Ref. [26], dashed line), IBM-1 (Ref. [32], dotted line), and AVM (solid line). Experimental data are taken: circles from [33], triangles from [35]. *b*—Expectation values of the quadrupole moment in the first excited states for Ru isotopes. Experimental data are taken from [33] except the triangles being taken from Ref [35].

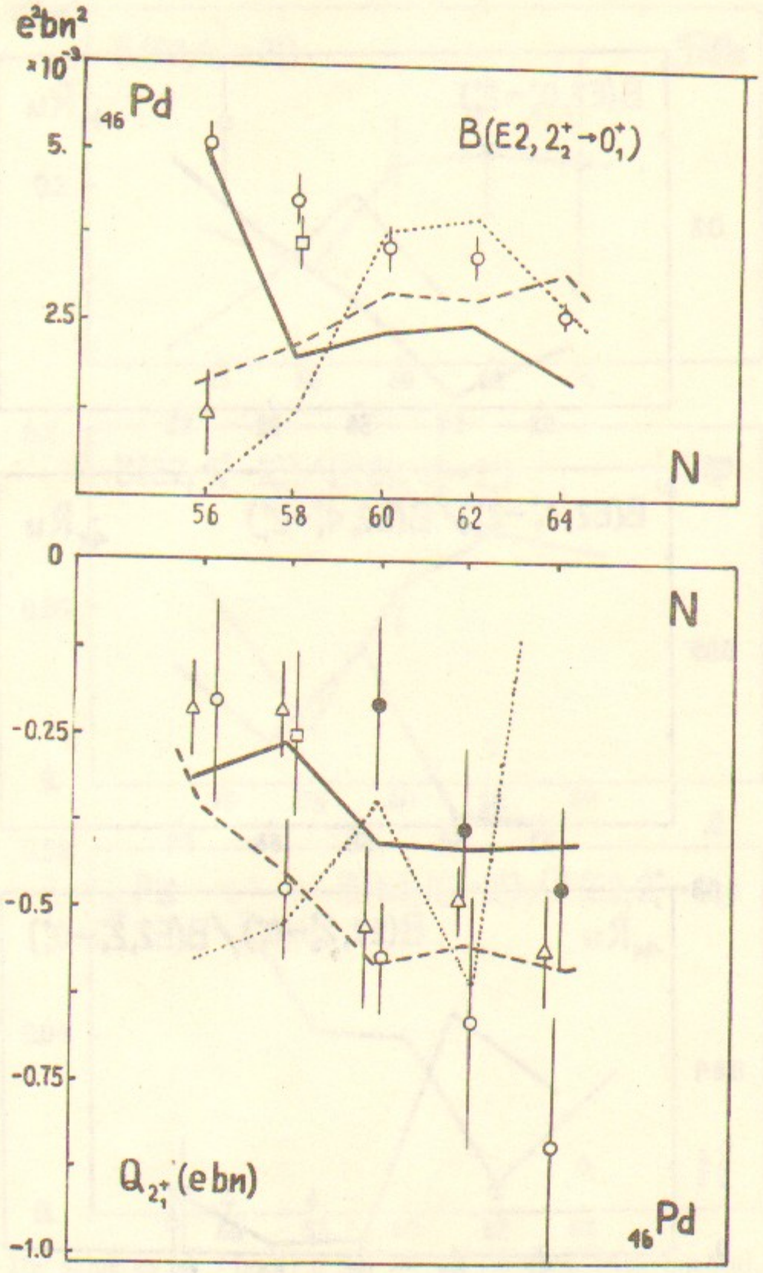

Fig. 18. a—The same as in Fig. 19,*a* but for Pd isotopes. Experimental data are taken: circles from [33], squares from [41]. *b*—The same as in fig. 19,*b* but for Pd isotopes. Experimental data are taken: closed circles from [2], others from [33].

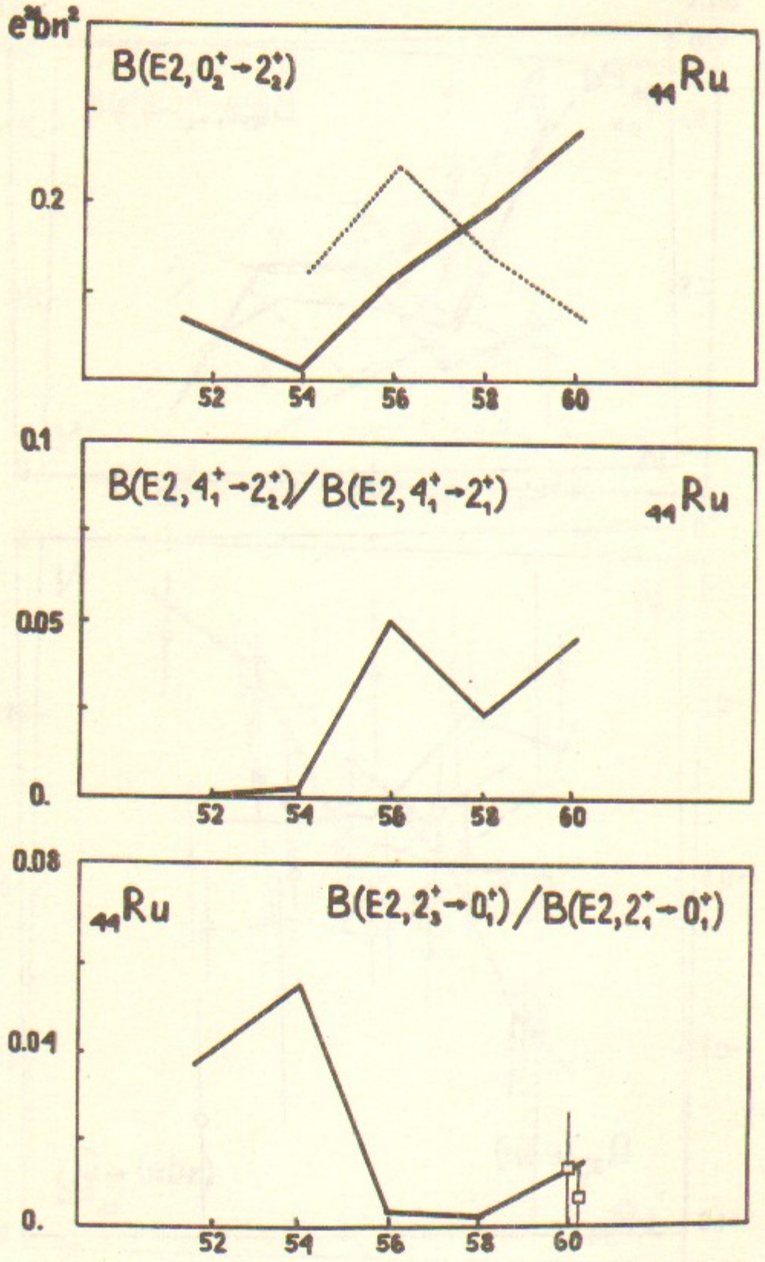

Fig. 19.
a—Absolute values of $B(E2; 0_2^+ \to 2_2^+)$ in Ru isotopes as predicted by the AVM. IBM-1—results (Ref. 32) are also presented.
b—Ratios $B(E2; 4_1^+ \to 2_2^+)/B(E2; 4_1^+ \to 2^+{}_1)$ in Ru isotopes as predicted by the AVM.
c—Ratios $B(E2; 2_3^+ \to 0_1^+)/B(E2; 2_1^+ \to 0^+{}_1)$ in Ru isotopes as predicted by the AVM. Experimental dots for ^{104}Ru are taken from Ref. [16].

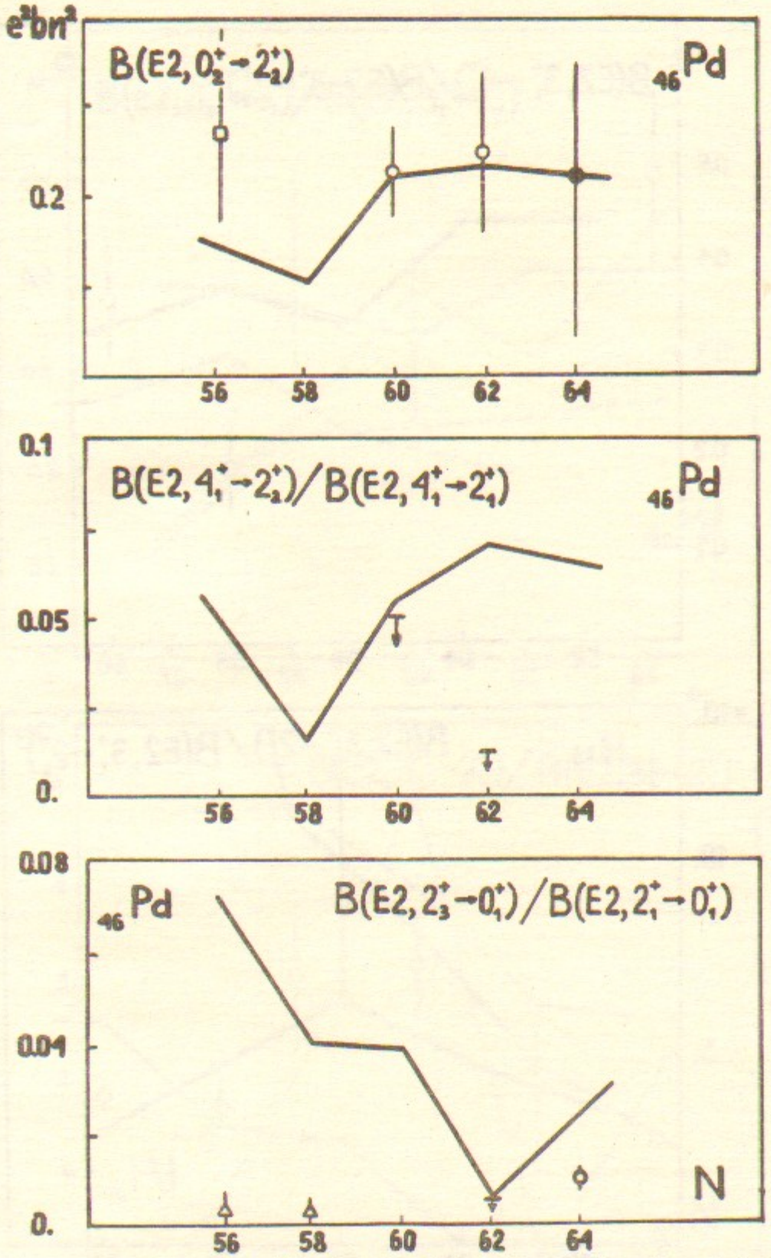

Fig. 20. *a*—The same as in Fig. 17,*a* but for Pd isotopes. Experimental data are taken: opened circles from [42]*), squares from [41], and closed circles from [28]. *b*—The same as in Fig. 17,*b* but for Pd isotopes. experimental estimates are taken from Ref. [42]. *c*—The same as in Fig. 17,*c* but for Pd isotopes. Exsperimental values are taken from [41] and [24], for the ^{108}Pd, the upper limit was taken from Ref. [45].

*) The ratios $B(E2; 0_2^+ \to 2_1^+)/B(E2; 0_2^+ \to 2_2^+)$, measured in Ref. [42], have been used by the author to calculate values of $B(E2; 0_2^+ \to 2_2^+)$.

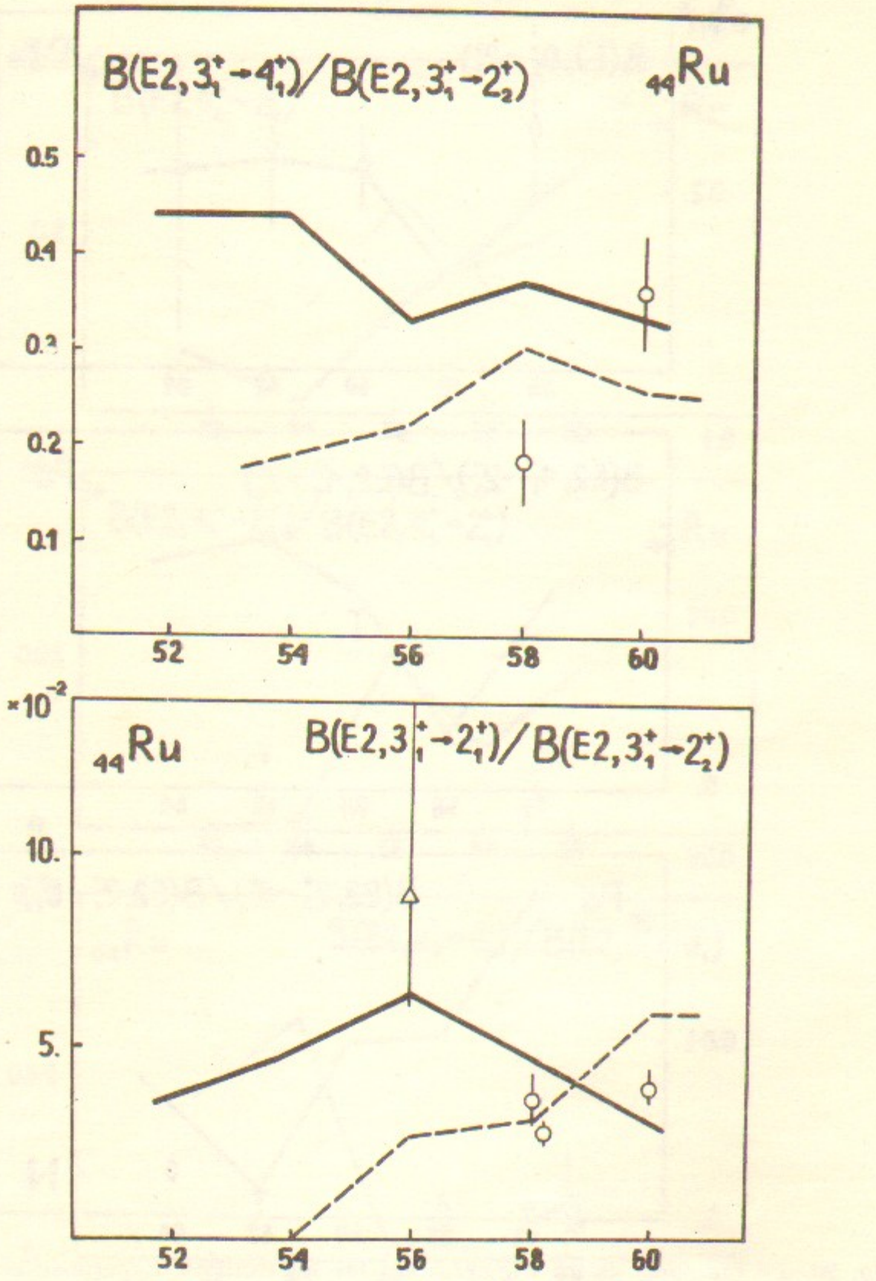

Fig. 21. a —Ratios $B(E2; 3_1^+ \to 4_1^+)/B(E2; 3_1^+ \to 2_2^+)$ in Ru isotopes and results of calculations in the IBM-2 (Ref. [26], dashed line) IBM-1 (Ref. [32], dotted line) and in AVM (solid line). Experimental data are taken from Ref. [26]. *b*—The same as in part *a*, but for the ratio $B(E2; 3_1^+ \to 2_1^+)/B(E2; 3_2^+ \to 2_2^+)$. Experimental data are taken circles from [26], triangles from [36].

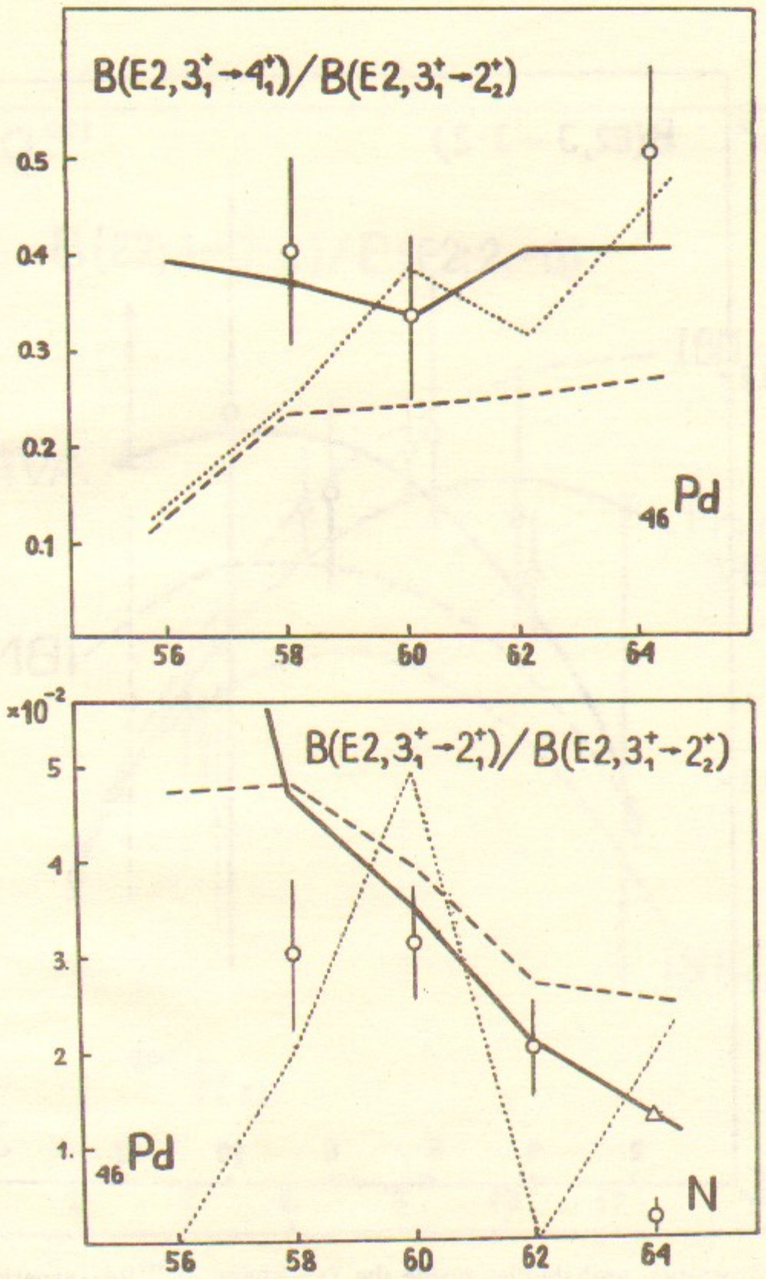

Fig. 22. a—The same as in Fig. 19,*a* but for Pd isotopes. *b*—The same as in Fig. 19,*b*, but for Pd isotopes. Experimental values are taken: circles from [26], triangles from [33].

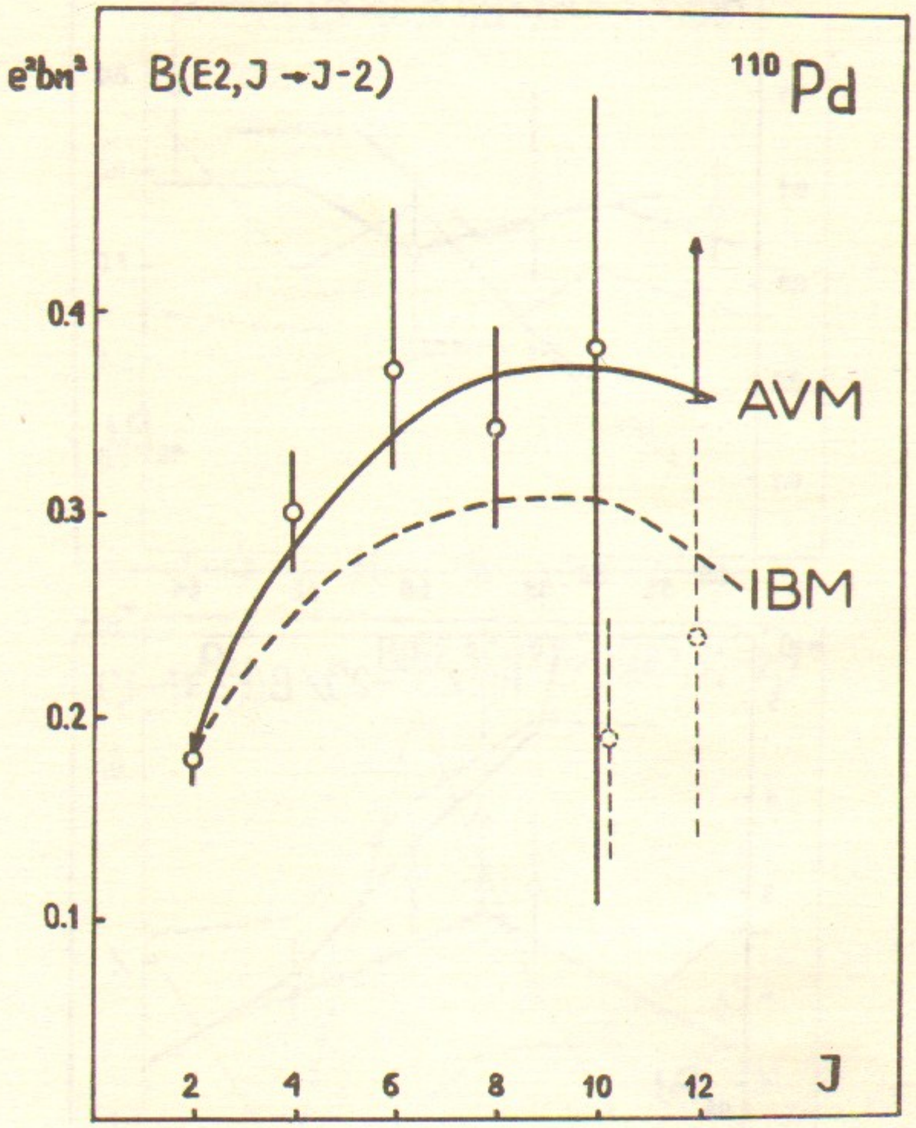

Fig. 23. E2-transition probabilities inside the Yrast-band of ^{110}Pd—experimental values (Ref. [28]) and theoretical ones calculated in the AVM (solid line) and in IBM (dashed line). Experimental bars marked with dashed lines correspond to levels of the Yrast- but not ground-state band.

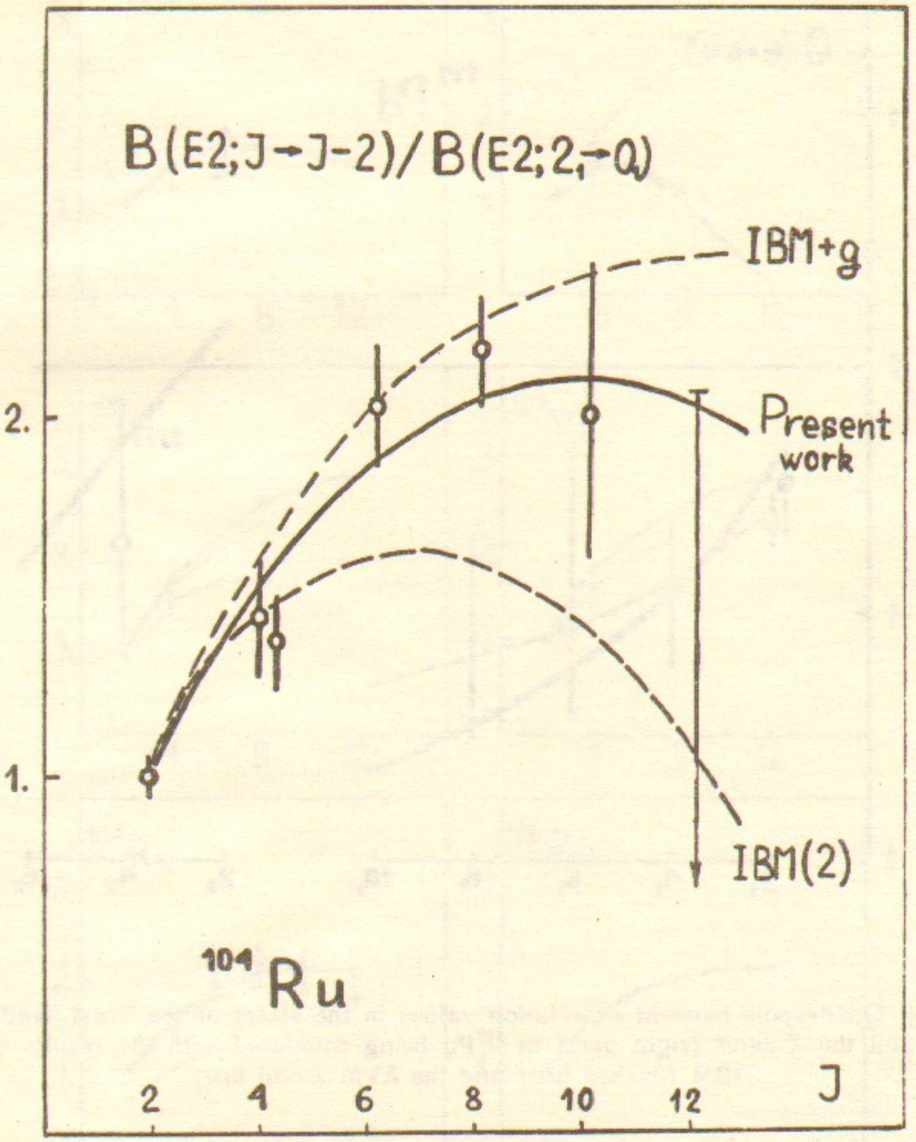

Fig. 24. The same as in Fig. 21, but for the ^{104}Ru, in units of $B(E2; 2^+_1 \rightarrow 0^+_1)$.

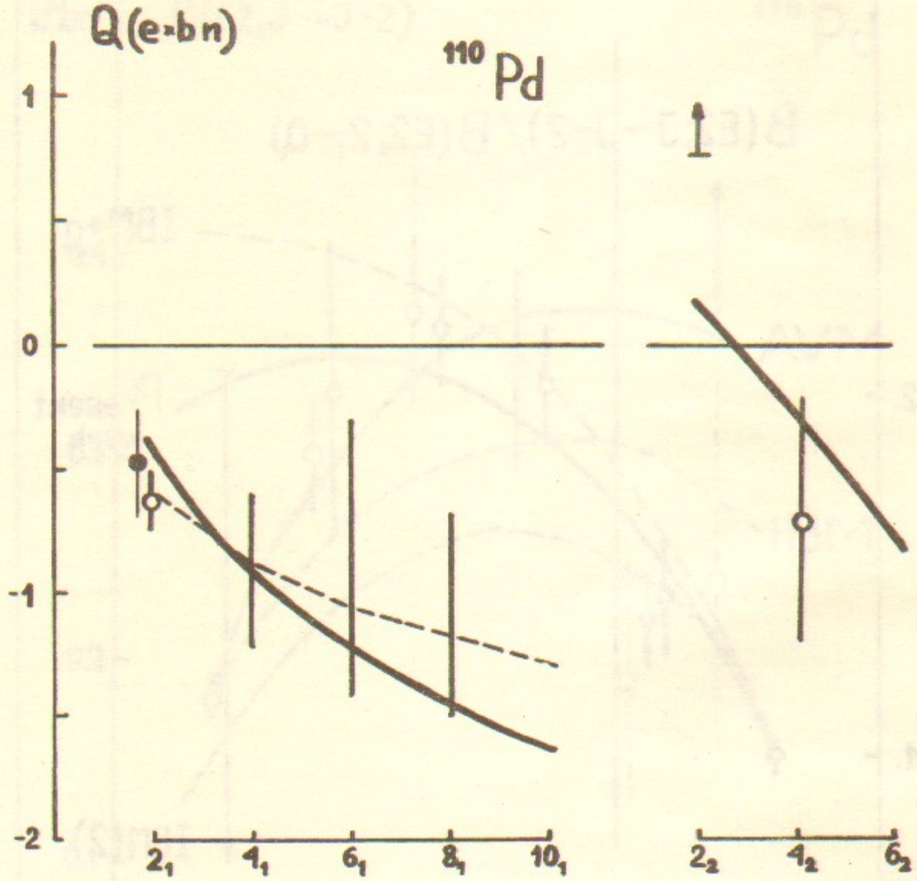

Fig. 25. Quadrupole moment expectation values in the states of the Yrast-band (left part) and the X-band (right part) in ^{110}Pd being compared with the results of the IBM (dashed line) and the AVM (solid line).

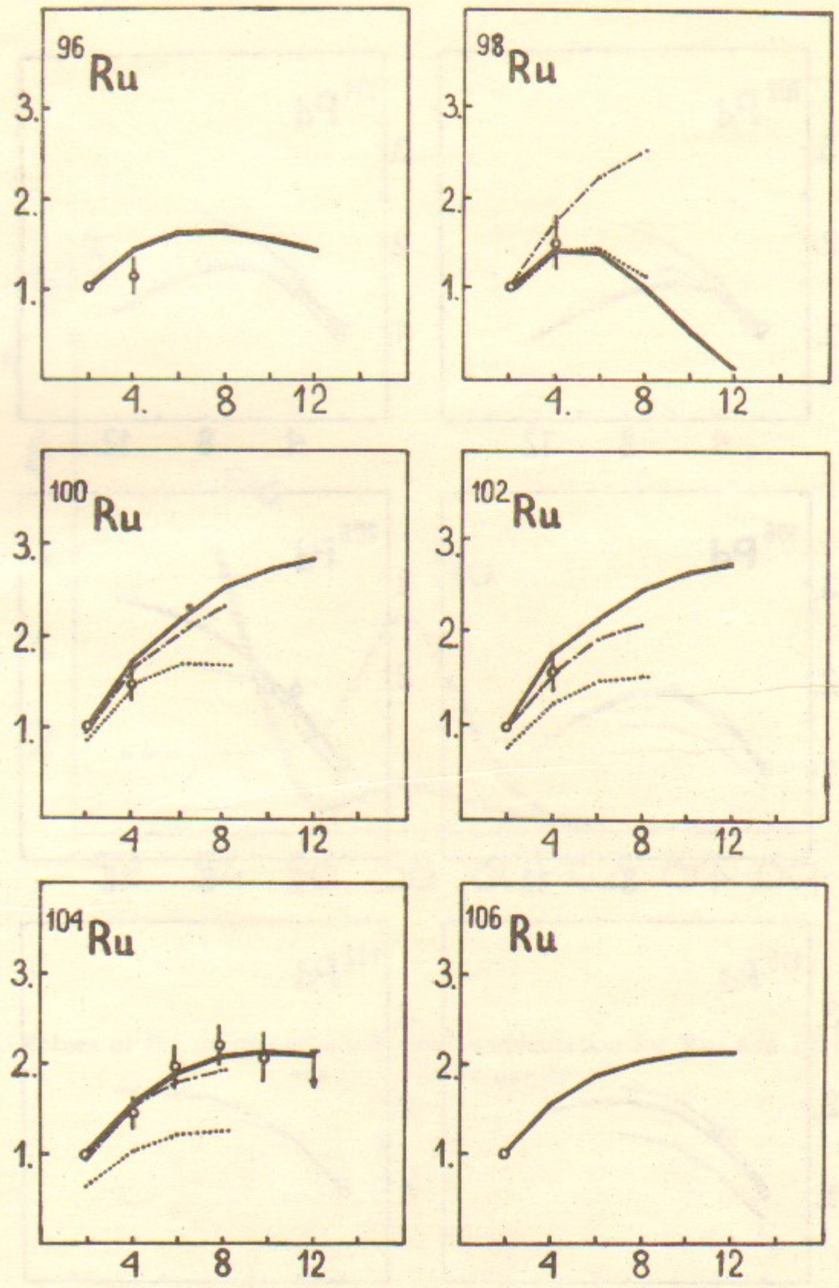

Fig. 26. Yrast-band E2-transition probabilities in Ru isotopes (normalized to $B(2_1^+ \to 0_1^+)$) as predicted by the AVM (solid line), IBM-1 (Ref. [32], dotted line), and BET (Ref. [33], dashed line). Experimental values are marked by circles.

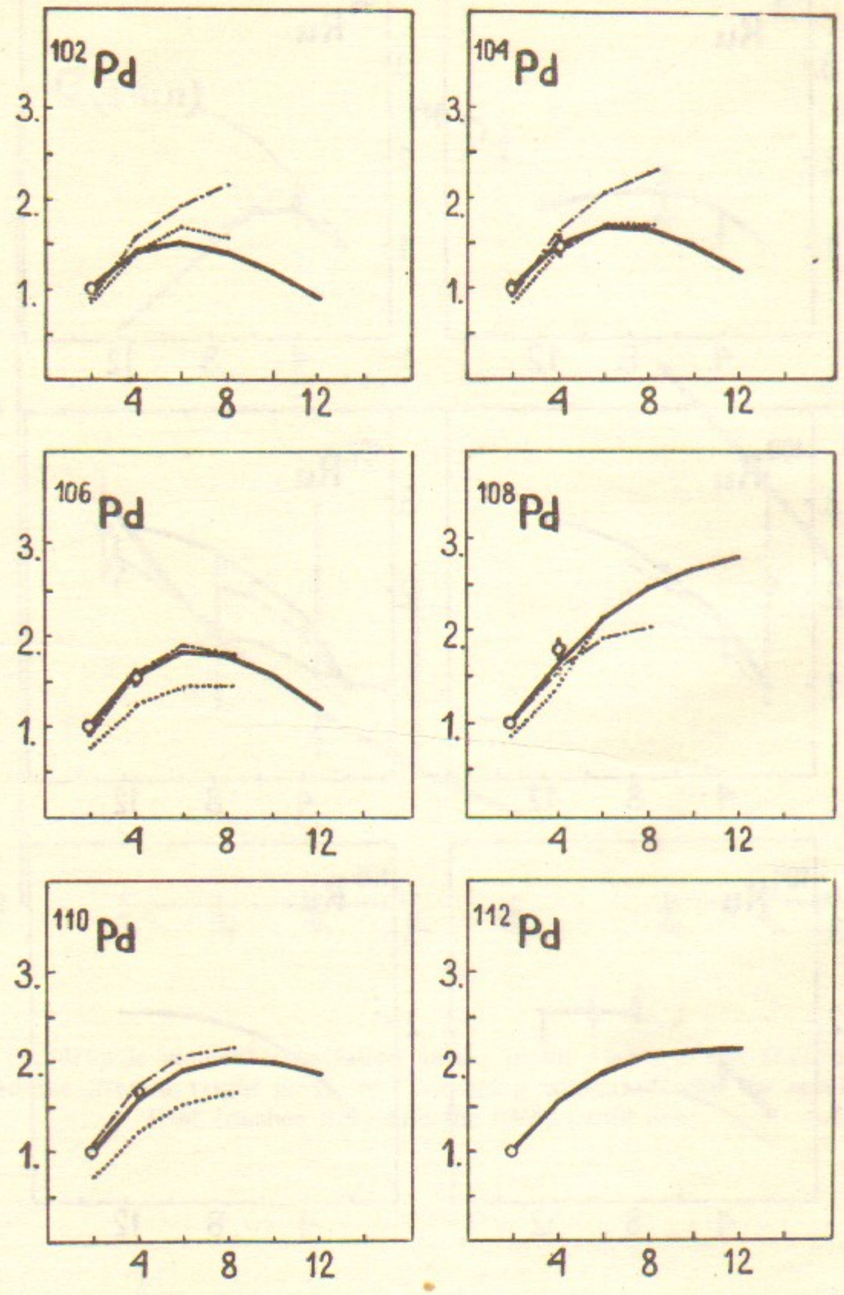

Fig. 27. The same as in Fig. 26 but for Pd isotopes.

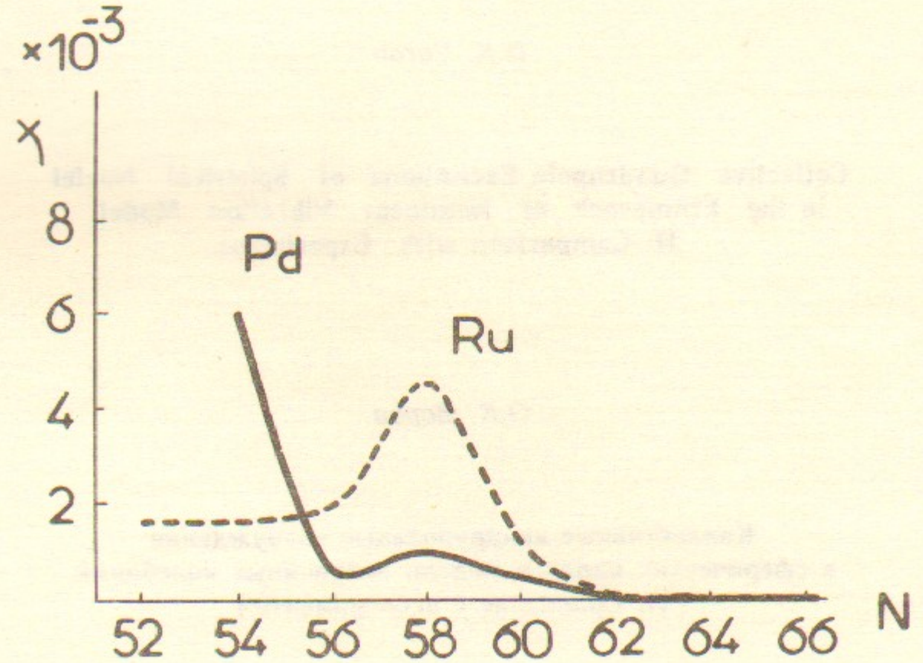

Fig. 28. Values of the parameter χ adopted to calculation for Ru- and Pd-chains versus the neutron number.

O.K. Vorov

Collective Quadrupole Excitations of Spherical Nuclei in the Framevork of Nonlinear Vibration Model. II. Comparison with Experiment.

O.K. Воров

Коллективные квадрупольные возбуждения в сферических ядрах в модели нелинейных колебаний. II. Сравнение с экспериментом

Ответственный за выпуск С.Г.Попов

Работа поступила 8 июля 1986 г.
Подписано к печати 18.11. 1986 г. МН 11867
Формат бумаги 60×90 1/16 Объем 3,8 печ.л., 3,0 уч.-изд.л.
Тираж 290 экз. Бесплатно. Заказ № 170

Набрано в автоматизированной системе на базе фотонаборного автомата ФА1000 и ЭВМ «Электроника» и отпечатано на ротапринте Института ядерной физики СО АН СССР.
Новосибирск, 630090, пр. академика Лаврентьева, 11.